# REACTION SYNTHESIS OF TITANIUM ALUMINIDE / TITANIUM DIBORIDE IN-SITU COMPOSITES

by

Elizabeth Ann Jeffers

Thesis submitted to the faculty of the
Virginia Polytechnic Institute and State University
in partial fulfillment of the requirements for the degree of

MASTER OF SCIENCE
in
Materials Science and Engineering

Approved by:

Dr. Stephen L. Kampe (Chair)
Dr. Kathryn V. Logan
Dr. Carlos T.A. Suchicital

September 28, 2006
Blacksburg, Virginia

Keywords: Reaction synthesis, SHS, In-Situ Composite, DSC, Titanium Aluminide, Titanium Diboride

**Reaction Synthesis of Titanium Aluminide / Titanium Diboride In-Situ Composites**

Elizabeth Ann Jeffers

ABSTRACT

Reaction synthesis is a processing technique where the thermal activation energy needed to form a compound is provided by the exothermic heat of formation of the thermodynamically stable product. This type of synthesis has been used to form a variety of ceramics, intermetallics, and in-situ composites. In this work, the effects of changing the stoichiometry of the titanium aluminide matrix, and the effects of extrinsic reaction variables on the behavior of the reaction were studied and compared to theoretical predictions. It was shown that changing the stoichiometry of the titanium aluminide did have an effect on the measured heat of reaction; however this did not match the prediction. Changing the extrinsic variables of titanium and aluminum particle sizes also showed a significant effect on the behavior of the reaction.

# Dedication

This work is dedicated to my grandfathers. Your lives have been and will always continue to be an inspiration to me.

Joseph M. Kulick – In Loving Memory

Michael F. Jeffers Sr.

# Acknowledgements

I would like to thank my advisor Dr. Stephen Kampe for his guidance and support throughout my research. I am also grateful to Dr. Kathryn Logan for her assistance in acquiring equipment needed for this research, for her suggestions and also for serving on my committee. And finally to Dr. Carlos Suchicital for his suggestions and for serving on my committee.

Thank you to Aerojet for providing me with the Aerojet Propulsion Fellowship for the 2005-2006 academic year.

Thank you to Matsys, Inc. for the SBIR funding that supported my project.

To Dr. Jeff Schultz, thank you for all of your technical assistance, suggestions, and patience.

To the Kamposites Research Group, it has been a joy working by your sides in the lab and getting to know each of you. Thank you for all of your suggestions, and even more so for your friendship.

A special thanks goes to David Berry and Michael Wooddell, whose senior design project laid the basis for a lot of my work and helped me develop my procedures and to lay the ground work for my program. David, a special thanks to you for all the help you've provided me with over the years.

To all of my friends, you have helped to keep me sane and enjoy my time at Virginia Tech. I would not be who I am without each of you.

Mom and Dad, thank you for all of your love and support throughout my life, and especially through this last bit. I hope you know how grateful I am for all that you have done and continue to do. I could not have done this without you. Michael and Brian, thank you for pushing me from the time I was born… I am stronger because of you.

Most importantly, I would like to thank my Lord and Savior, Jesus Christ. I am constantly in awe that you choose to bestow your grace and blessings upon me. May this work, and even more so my life, be glorifying to you.

# Table of Contents

# List of Figures

# List of Tables

# 0 Objectives

The purpose of this research is to examine the reaction synthesis of titanium aluminide / titanium diboride in-situ composites. Specifically, we seek to understand the effects of changing the stoichiometry of the titanium aluminide matrix, as well as the effects that extrinsic reaction variables have on the behavior of the reaction.

The specific goals of this work include:

- Estimate the maximum temperature and heat of reaction using published thermodynamic data
- Examine how maximum temperature and heat of reaction vary with changes in Ti-xAl and V% $TiB_2$ formulation, based on published thermodynamic variables
- Experimentally measure $T_{max}$ and $\Delta H_{rxn}$, and compare with computed results
- Investigate the effects of extrinsic reaction variables on the measured values.

# 1 Background

## 1.1 Reaction Synthesis

Reaction synthesis, or combustion synthesis, is a processing technique in which the thermal activation energy of formation of a compound is sustained by its exothermic heat of reaction [1, 2]. Reaction synthesis can be performed in two modes; self-propagating high-temperature synthesis (SHS) mode and thermal explosion or simultaneous combustion mode [1, 3-5].

In SHS mode a compact of the mixed constituent material is heated to ignition at a point after which the exothermic heat of formation reduces the kinetic barriers enabling the reaction to completion in a self-propagating manner [1-4, 6, 7]. In thermal explosion mode, the mixed constituent material is heated up in a furnace until the material reacts uniformly [3].

### 1.1.1 Thermodynamics of Reaction Systems

Since the underlying basis of reaction synthesis is the use of the high exothermicity of a reaction to facilitate formation of the thermodynamically stable product, [4] it is important to understand the thermodynamics of these reactions. Upon heating a blended mixture of reactants, the reaction will initiate ($T_{ig}$), and will release an amount of heat ($\Delta H_{rxn}$). The temperature increase is associated with the reduction in enthalpy that results from the reaction of reactants to a more thermodynamically preferred product form. The maximum temperature ($T_{max}$) can be in the range of 1000-6500K [4].

Both $\Delta H_{rxn}$ and $T_{max}$ can be calculated theoretically from temperature-dependent enthalpy curves of the reactant and product materials. Figure 1 shows a schematic diagram of the enthalpy curves that can be used to calculate the theoretical maximum temperature, also called the adiabatic temperature ($T_{Ad}$), and the theoretical heat of formation ($\Delta H_f$). $T_{Ad}$ is defined as the temperature at which the enthalpy of the products is equal to the enthalpy of the reactants at $T_{ig}$ (i.e. $H_r(T_{ig}) = H_p(T_{Ad})$). And $\Delta H_f$ is the difference of the reactant and product enthalpies at $T_{ig}$ (i.e. $\Delta H_f = H_r(T_{ig}) - H_p(T_{ig})$).

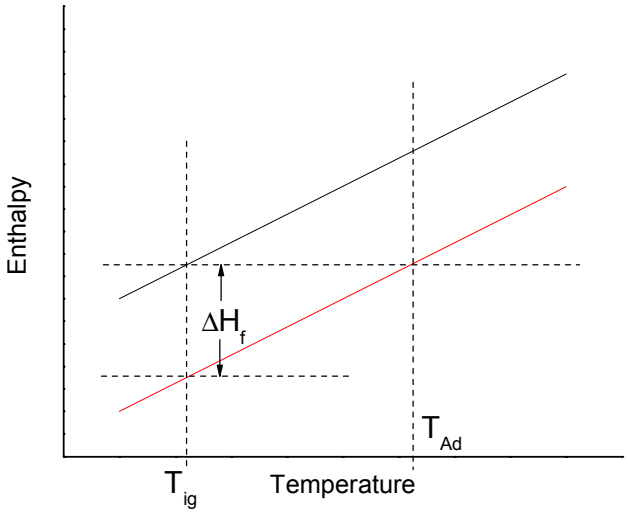


Figure 1: Schematic diagram of enthalpy curves for use in calculating $T_{Ad}$ and $\Delta H_f$ in a system with no phase changes.

### 1.1.2 Possible Reaction Systems

Reaction synthesis has been used to create many different materials for a diverse set of applications. Forms of this technique have been used to form a variety of ceramics, intermetallics, and ceramic/intermetallic/metal matrix composites. One specific application of an early reaction synthesis reaction is the thermite reaction, which was a reduction of a metal oxide powder with aluminum powder [4]. In their review article, Moore and Feng compiled a partial list of materials that have been produced by reaction synthesis shown in Table 1 [4]. It should be noted that the titanium aluminides are among materials not included in the list that have also been shown to form by reaction synthesis. Moore and Feng further classified some of the applications of these materials as follows:

- Abrasives, cutting tools and polishing powders
- Resistive heating elements
- Shape memory alloys
- High temperature intermetallic compounds
- Steel processing additives (i.e. nitrided ferroalloys)
- Electrodes for electrolysis of corrosive media
- Coatings for containment of liquid metals and corrosive media
- Powders for further ceramic processing
- Thin films and coatings

- Functionally graded materials
- Composite materials
- Materials with specific magnetic, electrical, or physical properties (Reprinted with the permission of J.J. Moore) [4].

| | |
|---|---|
| Borides | CrB, $HfB_2$, NbB, $TaB_2$, TiB, $TiB_2$, $LaB_6$, MoB, $MoB_2$, $MoB_4$, $Mo_2B$, WB, $W_2B_5$, $WB_4$, $ZrB_2$, VB, $V_3B_2$, $VB_2$ |
| Carbides | TiC, ZrC, HfC, NbC, SiC, $Cr_3C_2$, $B_4C$, WC, TaC, $Ta_2C$, VC, $Mo_2C$ |
| Nitrides | $Mg_3N_2$, BN, AlN, SiN, $Si_3N_4$, TiN, ZrN, HfN, VN, NbN, TaN, $Ta_2N$ |
| Silicides | $TiSi_3$, $Ti_5Si_3$, ZrSi, $Zr_5Si_3$, $MoSi_2$, $TaSi_2$, $Nb_5Si_3$, $NbSi_2$, $WSi_2$, $V_5Si_3$ |
| Aluminides | NiAl, CoAl, $NbAl_3$ |
| Hydrides | $TiH_2$, $ZrH_2$, $NbH_2$, $CsH_2$, $PrH_2$, $IH_2$ |
| Intermetallics | NiAl, FeAl, NbGe, $NbGe_2$, TiNi, CoTi, CuAl |
| Carbonitrides | TiC-TiN, NbC-NbN, TaC-TaN, ZrC-ZrN |
| Cemented carbides | TiC-Ni, TiC-(Ni, Mo), WC-Co, $Cr_3C_2$-(Ni, Mo) |
| Binary compounds | $TiB_2$-$MoB_2$, $TiB_2$-$CrB_2$, $ZrB_2$-$CrB_2$, TiC-WC, TiN-ZrN, $MoS_2$-$NbS_2$, $WS_2$-$NbS_2$ |
| Chalcogenides | MgS, $NbSe_2$, $TaSe_2$, $MoS_2$, $MoSe_2$, $WS_2$, $WSe_2$ |
| Composites | $TiB_2$-$Al_2O_3$, TiC-$Al_2O_3$, $B_4C$-$Al_2O_3$, TiN-$Al_2O_3$, TiC-$TiB_2$, $MoSi_2$-$Al_2O_3$, MoB-$Al_2O_3$, $Cr_2C_3$-$Al_2O_3$, 6VN-5$Al_2O_3$, $ZrO_2$-$Al_2O_3$-2Nb |

Table 1: A partial list of materials that have been produced via a reaction synthesis reaction (Reprinted with the permission of J.J. Moore) [4].

Benefits of utilizing reaction synthesis for materials processing include higher purity products, and less time and energy required to process the material [4, 7]. The main disadvantage for reaction synthesis is that the reaction product is typically porous, and thus requires additional processing if a bulk form is desired. Several new processing techniques have been examined in an attempt to incorporate densification along with the reaction to provide a dense product.

### 1.1.3 Methods of Reaction Synthesis

There are many different methods for conducting reaction synthesis reactions. Most center around the two modes of the reaction, SHS and thermal explosion. There have been many studies on the SHS and thermal explosion modes, as well as on methods to activate or ignite the reaction differently, along with other studies that have focused on densification of the product material.

In the SHS mode of reaction synthesis, ignition of a constituent powder blend typically occurs at a single point and spreads in a self-propagating manner to completion without any further external energy input. This is due to the fact that the energy released

from the reaction provides sufficient thermal energy to overcome the kinetic barriers associated with the reaction [1-4, 6, 7]. In thermal explosion mode the mixed constituent material is heated in a furnace until the material ignites uniformly [3].

Generally, explosion mode is used for reactions that do not self-propagate once initiated. Self-propagation is associated with high heats of reaction and high adiabatic temperatures. Merzhanov empirically concluded that for $T_{Ad} \leq 1800K$ reactions will not be self-propagating [7]. In order to assist initiation and propagation in reaction systems with $T_{Ad} \leq 1800K$, methods such as preheating, field activated SHS, and mechanically activated SHS have been developed [6]; however they fall outside the scope if this report and will not be discussed further.

# 2 Experimental Procedure

## 2.1 Selection of System

Reaction synthesis is a viable method for synthesizing many types of in-situ composites. Some possible matrix – reinforcement combinations were shown in Table 1 in Section 1.1.2. From previous experience it was decided that the reaction system would be a titanium aluminide matrix with titanium diboride reinforcement. Both titanium aluminide and titanium diboride have been studied independently. It has been shown that both are exothermic, and that $TiB_2$ is highly exothermic [7]. The nature of the titanium-aluminum system as the matrix component allows for a study of the effects of changing the titanium aluminide stoichiometry on the behavior of the reaction.

## 2.2 Thermodynamic-based Model / Predictions

A program was written in Matlab (Version 6.1.0.450 Release 12.1) to perform the needed theoretical calculations. A basic flowchart for the program layout is presented in Figure 2 followed by sections describing the subroutines. The program was written in such a way that the user can select the desired output. Several subroutines were written which perform a specific part of the necessary calculations for each of the desired outputs. They are discussed in the following sections, followed by the outputs.

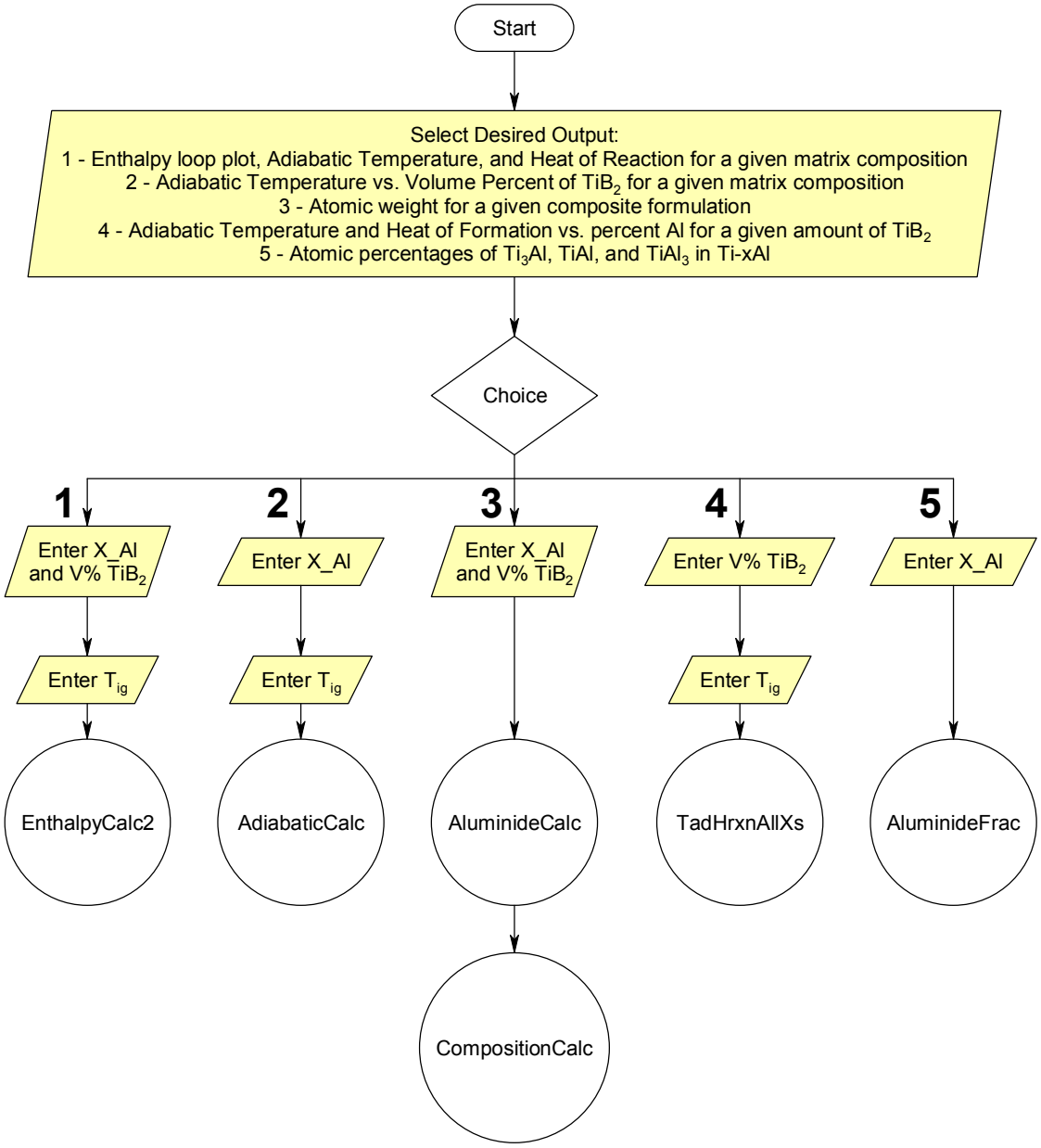


Figure 2: Basic flowchart of the main program that performs the theoretical calculations.

### 2.2.1 AluminideFrac Subroutine

The AluminideFrac subroutine calculates the atomic fractions of $Ti_3Al$, TiAl, and $TiAl_3$ in the matrix composition specified by the user. These calculations are inverse lever rule calculations based on the aluminum-titanium equilibrium phase diagram shown in Figure 3. An assumption was made for this study that the $TiAl_2$ phase between the TiAl and $TiAl_3$ regions on the phase diagram does not exist as its validity has not been well established. Therefore the end result of the off stoichiometric titanium aluminide is

assumed to be a combination of TiAl and either $Ti_3Al$ on the aluminum lean side, or $TiAl_3$ on the aluminum rich side. The assumed values for the locations of the phase regions at room temperature are shown in Table 2.

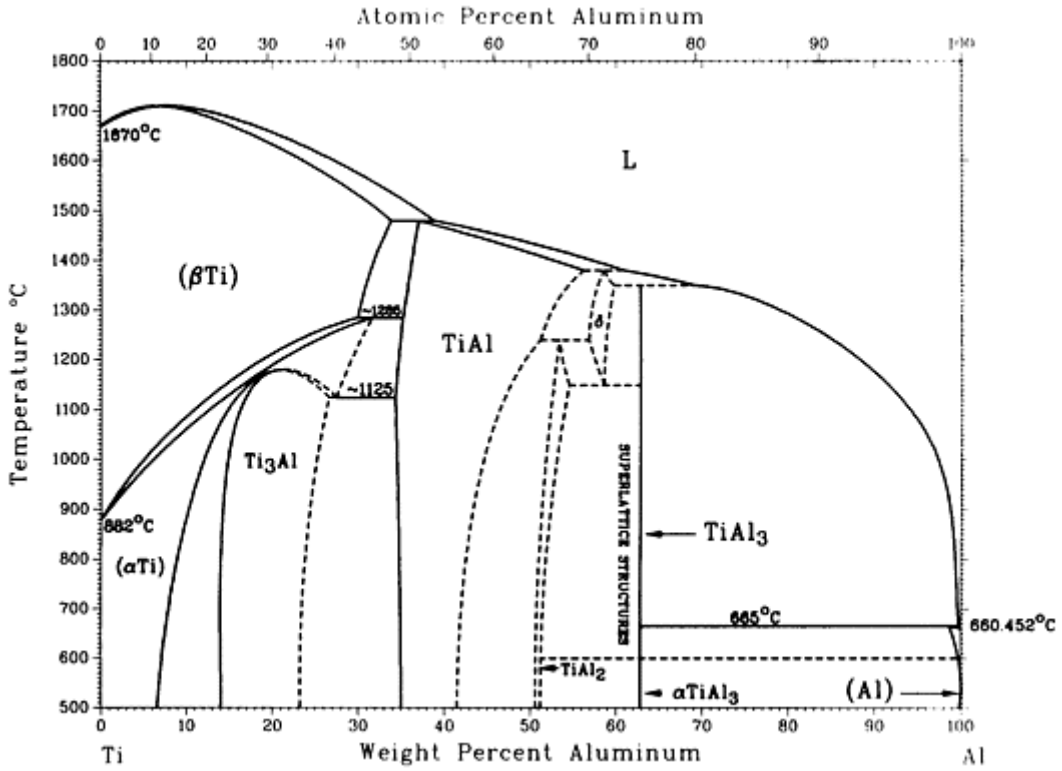


Figure 3: Aluminum-titanium equilibrium phase diagram [8]. Reprinted with permission of ASM International(r). All rights reserved. www.asminternational.org.

| Phase Region | At% Al |
|---|---|
| $Ti_3Al$ | 25 - 34 |
| $Ti_3Al$ + TiAl | 34 - 51 |
| TiAl | 51 - 57 |
| TiAl + $TiAl_3$ | 57 - 75 |

Table 2: Assumed phase region boundaries at room temperature.

For Ti-xAl compositions where $25 \leq x < 34$, the atomic fractions of the titanium aluminides are:

$$f_{\mathrm{Ti_3Al}} = 1$$
$$f_{\mathrm{TiAl}} = 0 \qquad (1)$$
$$f_{\mathrm{TiAl_3}} = 0$$

For Ti-xAl compositions in the range of $34 \leq x < 51$, the atomic fractions of the titanium aluminides are calculated as follows:

$$f_{\mathrm{Ti_3Al}} = \frac{51 - x}{51 - 34}$$
$$f_{\mathrm{TiAl}} = \frac{x - 34}{51 - 34} \qquad (2)$$
$$f_{\mathrm{TiAl_3}} = 0$$

For Ti-xAl compositions in the range of $51 \leq x < 57$ the atomic fractions of each component are:

$$f_{\mathrm{Ti_3Al}} = 0$$
$$f_{\mathrm{TiAl}} = 1 \qquad (3)$$
$$f_{\mathrm{TiAl_3}} = 0$$

Finally, for compositions in the range of $57 \leq x \leq 75$, the calculations are:

$$f_{\mathrm{Ti_3Al}} = 0$$
$$f_{\mathrm{TiAl}} = \frac{x - 57}{75 - 57} \qquad (4)$$
$$f_{\mathrm{TiAl_3}} = \frac{75 - x}{75 - 57}$$

### 2.2.2 AluminideCalc Subroutine

The AluminideCalc subroutine calculates the atomic weight and density of the user's desired matrix composition. To do so it calls the AluminideFrac subroutine and using rule-of-mixtures (ROM) calculates both the atomic weight and density of the Ti-xAl composition as follows:

$$\mathrm{AW_{Ti-xAl}} = f_{\mathrm{Ti_3Al}} \times \mathrm{AW_{Ti_3Al}} + f_{\mathrm{TiAl}} \times \mathrm{AW_{TiAl}} + f_{\mathrm{TiAl_3}} \times \mathrm{AW_{TiAl_3}}$$
$$\rho_{\mathrm{Ti-xAl}} = f_{\mathrm{Ti_3Al}} \times \rho_{\mathrm{Ti_3Al}} + f_{\mathrm{TiAl}} \times \rho_{\mathrm{TiAl}} + f_{\mathrm{TiAl_3}} \times \rho_{\mathrm{TiAl_3}} \qquad (5)$$

The atomic weights and densities for all of the constituents used in this study are shown in Table 3.

| | Atomic Weight, g/mol | Density, $g/cm^3$ |
|---|---|---|
| Ti | 47.9 | 4.5 |
| Al | 26.98 | 2.7 |
| B | 10.811 | 2.34 |
| $Ti_3Al$ | 170.68 | 4.2 |
| TiAl | 75.2 | 3.91 |
| $TiAl_3$ | 128.84 | 3.4 |
| $TiB_2$ | 69.522 | 4.5 |

Table 3: Atomic weights and densities of the constituents used in this study [9].

### 2.2.3 CompositionCalc Subroutine

For a user specified composite of Ti-xAl + yV% $TiB_2$, the CompositionCalc subroutine calculates the atomic fractions of Ti-xAl and $TiB_2$, and the theoretical atomic weight of the composite. The calculations for these are as follows:

$$n_{Ti-xAl} = \frac{(1-y)\times\rho_{Ti-xAl}}{AW_{Ti-xAl}}$$

$$n_{TiB_2} = \frac{(1-y)\times\rho_{TiB_2}}{AW_{TiB_2}}$$

$$n_{total} = n_{Ti-xAl} + n_{TiB_2}$$

$$f_{Ti-xAl} = \frac{n_{Ti-xAl}}{n_{total}}$$

$$f_{TiB_2} = \frac{n_{TiB_2}}{n_{total}}$$

$$AW_{composite} = f_{Ti-xAl}\times AW_{Ti-xAl} + f_{TiB_2}\times AW_{TiB_2} \quad (6)$$

where $n_Z$ is the number of moles of Z. The values for the atomic weight and density of $TiB_2$ are shown previously in Table 3.

### 2.2.4 abcdCalc Subroutine

The standard form of the chemical equation for this reaction is:

$$aTi + bAl + cB \rightarrow zTi\text{-}xAl + yTiB_2$$

where a, b, and c are the number of moles of titanium, aluminum, and boron respectively needed to for z moles of Ti-xAl and y moles of $TiB_2$. However, when performing the enthalpy calculations for this reaction system it is useful to write the chemical reaction equation as:

$$aTi + bAl + cTi + dB \rightarrow zTi\text{-}xAl + yTiB_2$$

where a and b are the number of moles of titanium and aluminum respectively needed to form z moles of Ti-xAl, c and d are the number of moles of titanium and boron needed to form y moles of $TiB_2$, and z and y are the number of moles of Ti-xAl and $TiB_2$ formed in the reaction (i.e. the atomic fractions of each that were calculated in the previous section). Assuming that one mole of the composite is formed (i.e. z+y = 1) a, b, c, and d can be calculated as:

$$\begin{aligned} a &= 2 \cdot (1 - x) \cdot f_{Ti-xAl} \\ b &= 2 \cdot x \cdot f_{Ti-xAl} \\ c &= f_{TiB_2} \\ d &= 2 \cdot f_{TiB_2} \end{aligned} \tag{7}$$

where x is the user specified amount of aluminum in Ti-xAl, and $at\%_{Ti\text{-}xAl}$ and $at\%_{TiB2}$ were calculated in Section 2.2.3.

### 2.2.5 EnthalpyCalc Subroutine

The EnthalpyCalc subroutine plots the enthalpy loop for Ti-xAl + yV% $TiB_2$ and calculates $T_{Ad}$ and $\Delta H_f$ for a user specified composition. The program allows the user to input $T_{ig}$ if it is known, or it will assume a value of 1000K.

The enthalpy loops are calculated from H(T) data for the products and reactants. The H(T) data used for these calculations is shown in Appendix A. It should be noted that there was no data available for $Ti_3Al$, therefore the data for $TiAl_3$ was used for it. This was assumed because in other $M_3Al$ systems, the $M_3Al$ H(T) data was similar to the $MAl_3$ H(T) data [10].

To ease the calculations in Matlab, best fit lines of the data between phase transitions were calculated using Microsoft Excel using the polynomial fit of each section until the $R^2 \geq 0.999$. The enthalpies of the products and reactants were calculated for a temperature range of 298-3500K using the following equations:

$$\Delta H_r(T) = a \cdot H_{Ti}(T) + b \cdot H_{Al}(T) + c \cdot H_{Ti}(T) + d \cdot H_B(T) \quad (8)$$

$$\Delta H_p(T) = f_{Ti_3Al} \cdot H(T)_{Ti_3Al} + f_{TiAl} \cdot H(T)_{TiAl} + f_{TiAl_3} \cdot H(T)_{TiAl_3} + f_{TiB_2} \cdot H(T)_{TiB_2} \quad (9)$$

$T_{Ad}$ and $\Delta H_f$ were calculated as described in Section 1.1.1.

### 2.2.6 AdiabaticCalc Subroutine

For a given matrix composition, the AdiabaticCalc subroutine calculates $T_{Ad}$ and $\Delta H_f$ across the whole volume percent $TiB_2$ range. To do so it performs the same calculations that were described in Section 2.2.5, but it loops from 0 to 100V% $TiB_2$.

### 2.2.7 TadHrxnAllXs Subroutine

For a given volume percent, the TadHrxnAllXs subroutine calculates $T_{Ad}$ and $\Delta H_f$ across the range of aluminum concentrations. The calculations are performed in the same manner as in Section 2.2.5 at aluminum concentrations from 25at% to 75at%.

## 2.3 Formulations

Testing of two types of formulations was performed: monolithic formulations which are shown in Section 2.3.1 and composite formulations which are shown in Section 2.3.2. The particle sizes of the titanium, aluminum, and boron powders used in the monolithic and composite formulation powder blends were analyzed in a Horiba LA950 Particle Size Analyzer.

### 2.3.1 Monolithic Formulations

The three elemental constituents as well as blends to form TiAl and $TiB_2$ were individually tested in the Differential Scanning Calorimeter (DSC) using the procedure that will be shown in Section 2.4.2. For these experiments the constituents used were: titanium powder (-325 mesh, 99.7% pure, Atlantic Equipment Engineers), aluminum powder (-100 mesh, 99.8% pure, Atlantic Equipment Engineers), and amorphous boron powder (>1μm, 99% pure, Atlantic Equipment Engineers). Table 4 shows the formulations used for the TiAl and $TiB_2$ experiments.

| Formulation | wt% Ti | wt% Al | wt% B |
|---|---|---|---|
| TiAl | 63.969 | 36.031 | 0 |
| $TiB_2$ | 68.899 | 0 | 31.101 |

Table 4: Formulations for TiAl and $TiB_2$ experiments.

### 2.3.2 Composite Blend Formulations

The Ti-xAl + 40V% $TiB_2$ general composition was selected for the study of changing the aluminide stoichiometry. For these experiments the constituents used were: titanium powder (-325 mesh, 99.7% pure, Atlantic Equipment Engineers), aluminum powder (-100 mesh, 99.8% pure, Atlantic Equipment Engineers), and amorphous boron powder (>1μm, 99% pure, Atlantic Equipment Engineers).

To study the effect of changing the stoichiometry of the titanium aluminide matrix, reactant formulations were calculated based on a titanium/aluminum atomic ratio, i.e. Ti-34Al is 34 at% aluminum in the titanium aluminide. As described in Section 2.2.1, the off stoichiometric titanium aluminide is assumed to be a combination of TiAl and either $Ti_3Al$ on the aluminum lean side, or $Al_3Ti$ on the aluminum rich side.

To see the effect that changing the stoichiometry of the titanium aluminide several compositions were selected and are shown in Table 5 along with the atomic percentages of $Ti_3Al$, TiAl, and $Al_3Ti$ in the matrix. To remain consistent each was formulated to form a product of Ti-xAl + 40V% $TiB_2$.

| Formulation | Atomic percent in Matrix | | | Weight Percentage | | |
|---|---|---|---|---|---|---|
| | $Ti_3Al$ | TiAl | $Al_3Ti$ | Ti | Al | B |
| Ti-25Al + 40V%$TiB_2$ | 100 | 0 | 0 | 77.704 | 9.101 | 13.195 |
| Ti-34Al + 40V%$TiB_2$ | 100 | 0 | 0 | 73.774 | 12.73 | 13.496 |
| Ti-42Al + 40V%$TiB_2$ | 52.94 | 47.06 | 0 | 70.085 | 16.136 | 13.779 |
| Ti-50Al + 40V%$TiB_2$ | 5.88 | 94.12 | 0 | 66.201 | 19.723 | 14.076 |
| Ti-58Al + 40V%$TiB_2$ | 0 | 94.44 | 5.56 | 62.101 | 23.508 | 14.39 |
| Ti-66Al + 40V%$TiB_2$ | 0 | 50 | 50 | 57.772 | 27.507 | 14.721 |
| Ti-75Al + 40V%$TiB_2$ | 0 | 0 | 100 | 52.597 | 32.285 | 15.118 |

Table 5: Matrix compositions and weight percentages of constituents for composite formulations.

These formulations were to be tested in the furnace and DSC using the procedures described in Sections 2.4.1 and 2.4.2.

## 2.4 Reaction Measurements

Two types of measurements were performed on each composite formulation: the measurement of the maximum temperature of the reaction, described in Section 2.4.1; and measurement of the heat of reaction using the DSC described in Section 2.4.2.

### 2.4.1 $T_{max}$ Measurements

Upon the selection of the reaction system, the following process was utilized to reaction synthesize the composites and measure the maximum temperature of the reaction:

1) The constituent powder mixture was formulated according to the desired matrix stoichiometry and reinforcement volume percent.
2) The powders were blended in a Nalgene bottle, without milling media, on a rolling mill to create a homogeneous mixture.
3) Specimens comprised of 10g of blended powder were pressed into cylindrical pellets 19.5 mm (0.75 inches) in diameter using a steel die in a uniaxial hydraulic press at a pressure of 195.08 MPa (22.2 ksi).
4) The constituent pellets were placed on a mullite refractory brick in a preheated 1000˚C (727 K) furnace with an open air environment. A Mikron Infrared M780 two-color infrared pyrometer with a published response time of 7.5 ms, and a temperature range of 1100˚C to 3700˚C, was aimed at the pellet to measure the maximum temperature of the reaction.

### 2.4.2 DSC Measurements

The experiments to measure the DSC response of the reaction were conducted in a similar manner to the maximum temperature experiments. Following steps 1 and 2 from the previous section the procedure continues as:

3) 1g of blended powder was pressed into cylindrical pellets 12.7 mm (0.5 inches) in diameter using a steel die in a uniaxial hydraulic press at a pressure of 702.3 MPa (101.9 ksi).
4) The constituent pellets were sectioned into specimens 10±0.5 mg in mass, and placed into an alumina crucible with a lid.

5) The alumina crucible was placed in the NETZSCH STA 449C differential scanning calorimeter with a bottled air atmosphere and heated at a rate of 40K/min up to 1050˚C (777 K).

#### 2.4.2.1 DSC Measurements for Ignition Experiment

To test the assumption that the ignition of the reaction occurs upon aluminum melting, steps 1-4 were followed as described in Section 2.4.2. Two experiments were run using a modified heating profile. In the first experiment step 5 was modified to:

5) The alumina crucible was placed in the NETZSCH STA 449C with a bottled air atmosphere and heated at a rate of 40K/min up to 750˚C and held for 20 minutes.

In the second experiment step 5 was modified to:

5) The alumina crucible was placed in the NETZSCH STA 449C with a bottled air atmosphere and heated at a rate of 40K/min up to 750˚C and held for 20 minutes followed by a 40K/min ramp up to 1150˚C.

## 2.5 Extrinsic Reactant Variables

Since the literature has indicated that extrinsic variables; such as powder particle size/shape, compaction density, and heating rate have an effect on the behavior of the reaction, it is important to gain an understanding of some of these specific effects within the titanium aluminide / titanium diboride reaction system. To do so, a Taguchi array was set up to look at the effects of titanium and aluminum particle size on the reaction behavior. Table 6 shows the L4 Taguchi array used for this purpose. Two compositions were selected for this test array: Ti-50Al + 20V% $TiB_2$; and, Ti-50Al + 40V% $TiB_2$. The formulations for these compositions are shown in Table 7. The materials used for these experiments are -325 mesh titanium powder (99.7% pure, Atlantic Equipment Engineers), -100 mesh titanium powder (99.7% pure, Atlantic Equipment Engineers), H10 aluminum powder (99.7% pure, Valimet), -100 mesh aluminum powder (99.8% pure, Atlantic Equipment Engineers), and amorphous boron powder (>1μm, 99% pure, Atlantic Equipment Engineers).

| Trial # | Aluminum Particle Size | Titanium Particle Size |
|---|---|---|
| 1 | H10 | -325 mesh |
| 2 | H10 | -100 mesh |
| 3 | -100 mesh | -325 mesh |
| 4 | -100 mesh | -100 mesh |

Table 6: Taguchi L4 array used to test the effects of varying aluminum and titanium particle size on the reaction output.

| Formulation | Weight Percentage | | |
|---|---|---|---|
| | Ti | Al | B |
| Ti-50Al + 20V%$TiB_2$ | 65.074 | 27.954 | 6.972 |
| Ti-50Al + 40V%$TiB_2$ | 66.115 | 20.350 | 13.535 |

Table 7: The reactant formulations for Taguchi L4 array.

These experiments were run in the furnace and DSC using the procedure described in Sections 2.4.1 and 2.4.2

# 3 Results and Discussion

This chapter presents the results of the predictions and experiments and explains the observed results.

## 3.1 Thermodynamic-based Model / Predictions

Theoretical calculations were performed to predict the behavior of the Ti-xAl + yV% $TiB_2$ composite system with varying aluminide and reinforcement content. Each of the predictions in this section was calculated assuming an ignition temperature of 1000K.

Figure 4 shows the enthalpy diagram for Ti-34Al + 40V% $TiB_2$. Shown on the diagram are $T_{Ad}$ and $\Delta H_f$ for this composition.

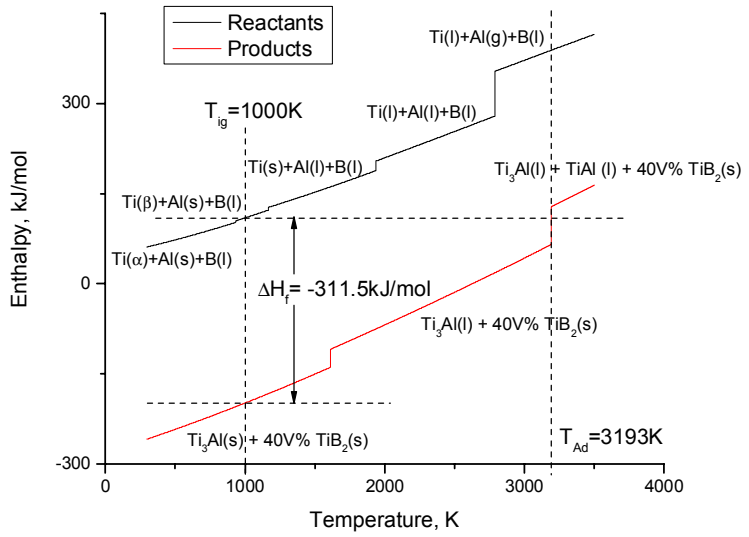


Figure 4: Enthalpy diagram for Ti-34Al + 40V% $TiB_2$ showing $T_{Ad}$ and $\Delta H_f$.

In Figure 5 the results of the calculations for how $T_{Ad}$ (assuming $T_{ig}$ = 1000K) varies across aluminide stoichiometry are shown for composites with 0, 10, 20, 30, 40 and 100V% $TiB_2$. $T_{Ad}$ increases with increasing amounts of $TiB_2$. In the case where there is 0V% $TiB_2$, the adiabatic temperature is that of just the Ti-xAl. The reason for the plateaus in that curve is that the melting temperature of TiAl is greater that those of $Ti_3Al$ and $TiAl_3$.

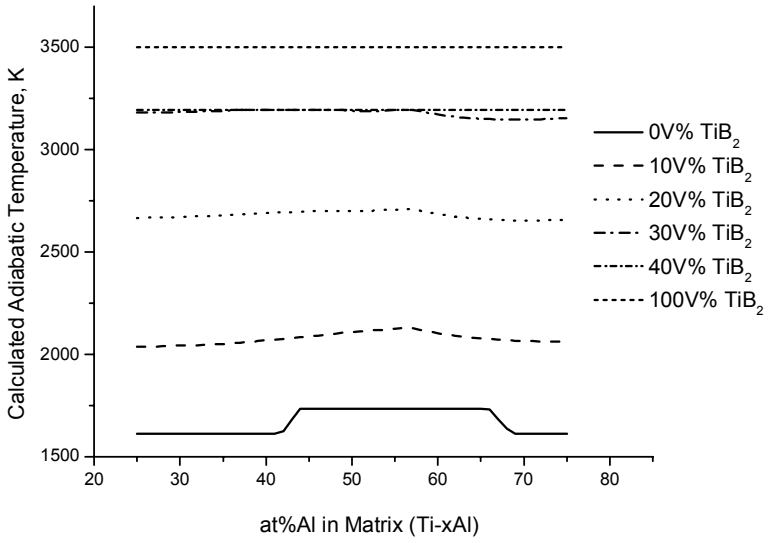


Figure 5: Theoretically calculated $T_{Ad}$ across the aluminum range.

Figure 6 shows the calculated results for $\Delta H_f$ across the aluminum content range for 0, 20, 40, 60, 80, and 100 V% $TiB_2$ in Ti-xAl. With the increasing amounts of $TiB_2$ $\Delta H_f$ becomes more exothermic, approaching the behavior of pure $TiB_2$ at high reinforcement percentages.

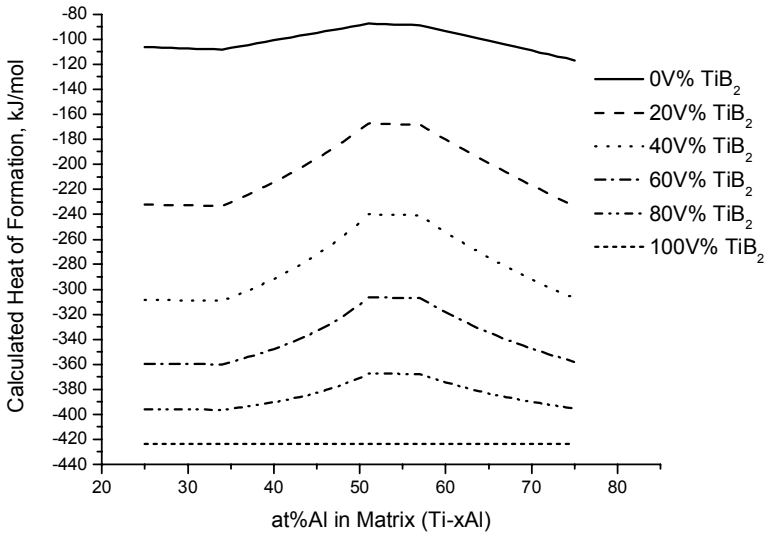


Figure 6: Theoretically calculated $\Delta H_f$ across the aluminum range.

Figure 7 presents the predictions of $T_{Ad}$ across the range of reinforcement percentage for matrix compositions of Ti-25Al ($Ti_3Al$), Ti-51Al (TiAl), and Ti-75Al

($TiAl_3$). For all three matrix compositions increasing amounts of $TiB_2$ increases $T_{Ad}$, the plateaus in the curves are associated with the thermal arrest that occurs during the melting of a constituent. Though the same thermodynamic data was used to calculate the Ti-25Al and Ti-75Al curves, they are distinctly different because the atomic weights of $Ti_3Al$ and $TiAl_3$ are different and the adiabatic temperature calculation is inherently dependent on atomic weight.

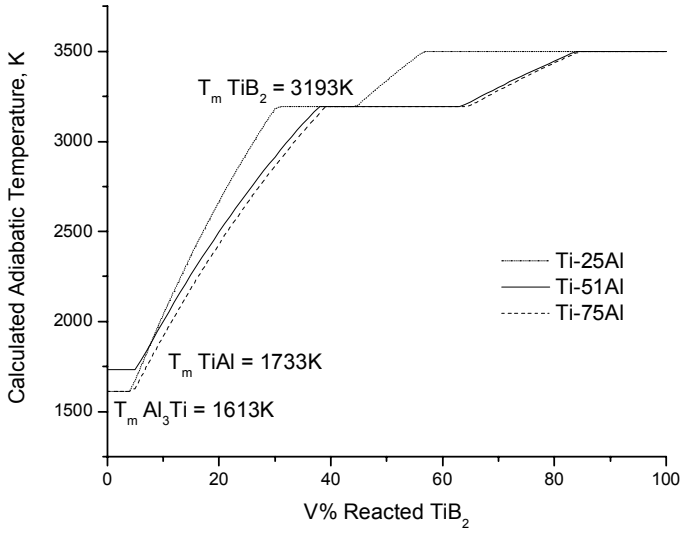


Figure 7: $T_{Ad}$ versus V% $TiB_2$ for Ti-25Al, Ti-51Al, and Ti-75Al matrix composites.

## 3.2 Formulations

The reaction behavior of varying formulations was measured to understand the effect of the changing formulation and its relation to the theoretical. The average particle sizes of the elemental powder constituents are presented in Table 7. For the discussion of the formulations, the average particle size will be used to identify the powder used in the blend.

| | Purity | Average Particle Size, µm | Standard Deviation, µm |
|---|---|---|---|
| Valimet H10 Al | 99.7% | 16.17 | 6.27 |
| AEE* -100 mesh Al | 99.8% | 127.63 | 67.24 |
| AEE* -325 mesh Ti | 99.7% | 46.27 | 18.21 |
| AEE* -100 mesh Ti | 99.7% | 99.00 | 51.69 |
| AEE* >1µm B | 99% | 0.345 | 0.105 |

Table 8: Particle sizes of the titanium, aluminum, and boron powders used in the monolithic and composite formulation blends. (*AEE – Atlantic Equipment Engineers)

### 3.2.1 Monolithic Formulations

In this section the results from the DSC experiments on monolithic formulations are presented and discussed. Section 3.2.1.1 presents the results of the elemental constituents and Section 3.2.1.2 presents the results of the TiAl and $TiB_2$ experiments.

#### 3.2.1.1 Elemental Constituents

To be confident in the analysis of the composite formulations it is important that the behavior of each of the elemental constituents is observed so that when are all combined together for reaction, the behavior can be attributed to the constituents or to the reaction. To achieve this goal, the titanium, aluminum and boron powders were each subjected to the temperature profile used in the reaction experiments in an air environment. Figure 8, Figure 9, and Figure 10 show the DSC and TG curves for titanium, aluminum, and boron respectively. The titanium curve exhibits an exotherm around 760˚C, the aluminum curve exhibits an endotherm around 670˚C and a small exotherm around 1000˚C, and the boron curve exhibits an exotherm around 600˚C. The increasing TG corresponding with the exotherm in each case is likely due to the oxidation of the material.

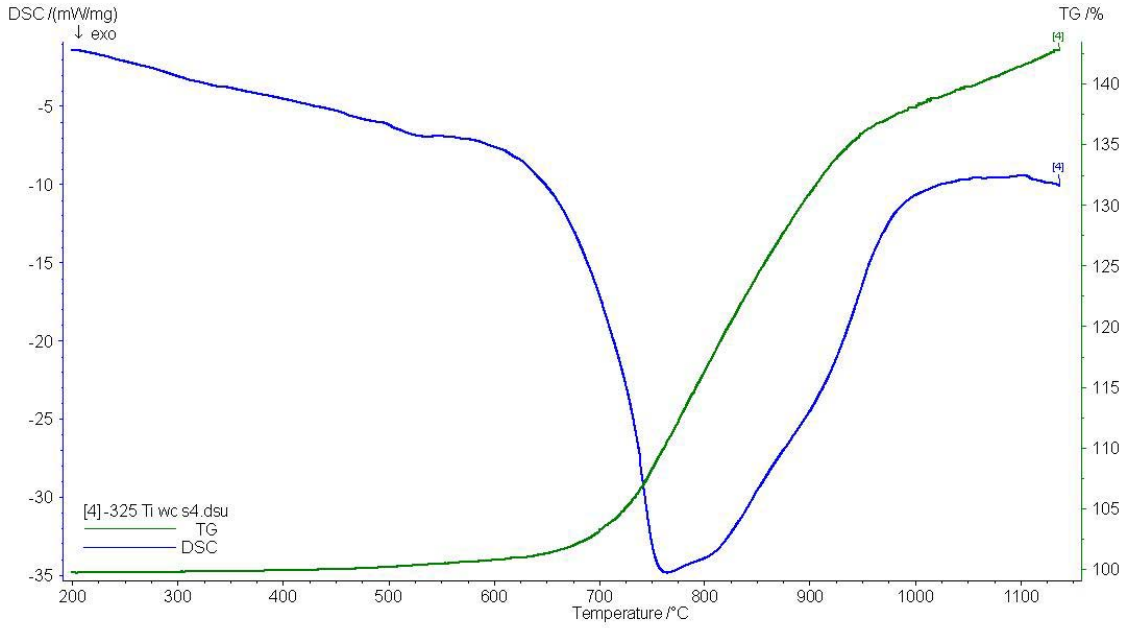


Figure 8: DSC and TG curves of 46µm titanium powder in air. An exotherm initiates at approximately 600°C and corresponds to an increase in mass suggesting oxidation of the titanium.

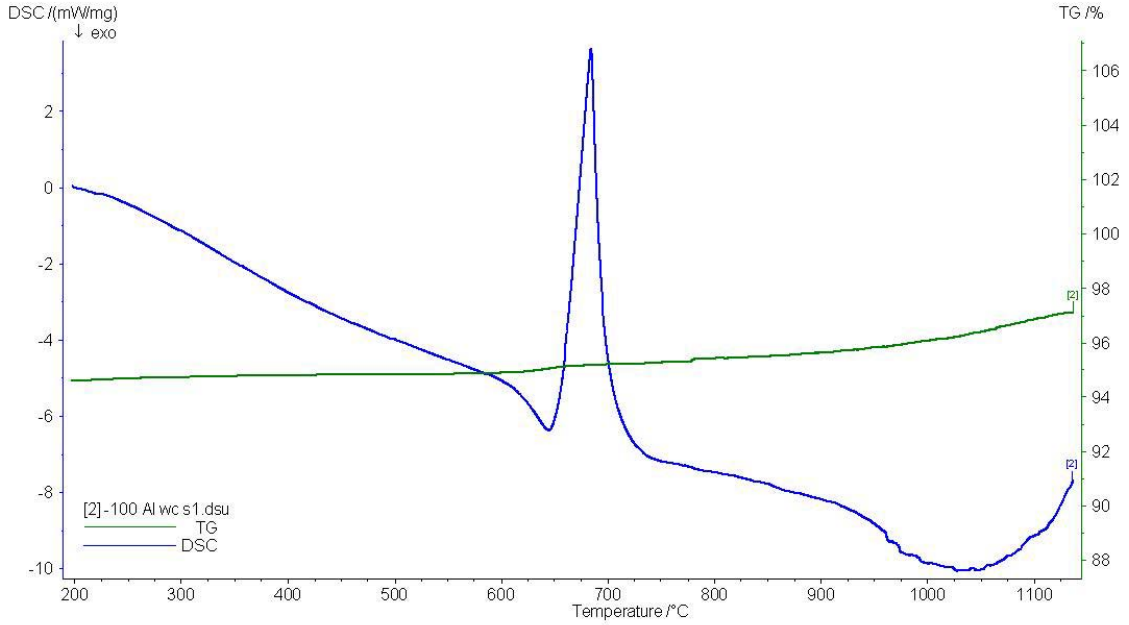


Figure 9: DSC and TG curves for 128µm aluminum powder in air. An endotherm initiates at approximately 630°C and corresponds to the melting temperature of aluminum. An exotherm initiates at approximately 950°C. The gradual increase in mass suggests oxidation of the aluminum.

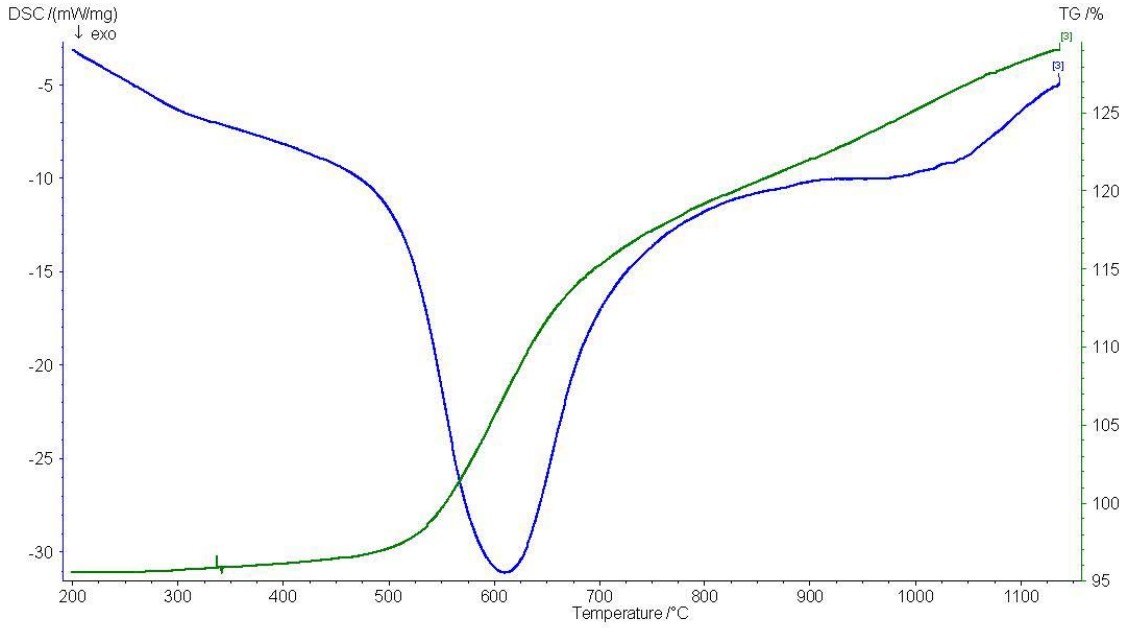


Figure 10: DSC and TG curves for 0.35µm amorphous boron in air. An exotherm initiates at approximately 500°C and corresponds to an increase in mass suggesting oxidation of the boron.

### 3.2.1.2 Composite Component Blends

Similarly to the characterization of the elemental constituents, blends were formulated to see if TiAl and $TiB_2$ would form independently under the standard heating profile. Figure 11 shows the DSC and TG curves for the TiAl experiment formulated with 128µm Al and 46µm Ti. Figure 12 shows the DSC and TG curves for the $TiB_2$ experiment formulated with 46µm Ti and 0.35µm B.

In Figure 11 we can distinctly see the aluminum melting endotherm followed by a two-humped exotherm. In the corresponding TG curve it can be seen that the material increased in weight following the melting of the aluminum. The endotherm and the latter exotherm appear to be from the aluminum, while the exotherm following the aluminum melting endotherm appears to be in the same location as the exotherm from the elemental titanium. Therefore, by comparison of this curve to the curves for the elemental aluminum and titanium we see that this curve appears to be the combination of the behaviors of titanium and aluminum as opposed to the formation of titanium aluminide. This was expected as $T_{Ad}$ for TiAl is 1733K which, by the Merzhanov criterion [7], is not expected to react spontaneously.

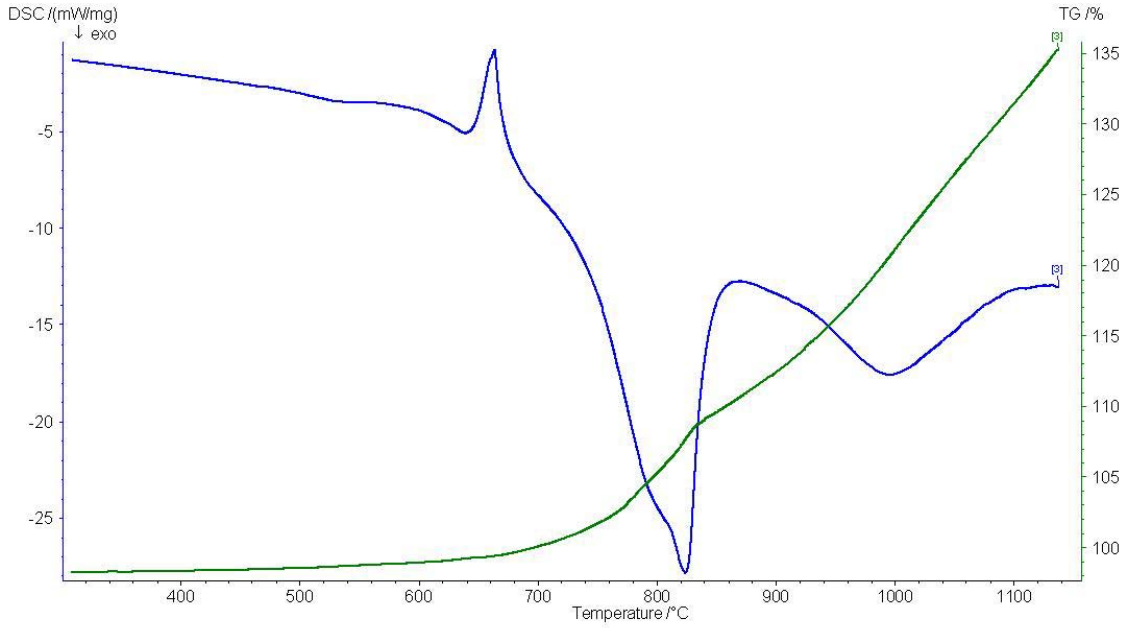


Figure 11: DSC and TG curves for TiAl formulated from 46µm Ti and 128µm Al reacted in air. The endotherm at approximately 630˚C and exotherm at approximately 950˚C correspond to the pure aluminum DSC curve, and the exotherm at approximately 600˚C corresponds to the titanium DSC curve. The distinct features indicate that no reaction occurred.

As for the $TiB_2$ experimental results shown in Figure 12, when compared to the elemental titanium and boron curves we can see that the curve appears very similar to that of the elemental amorphous boron curve, while no trace of the titanium behavior is noticed. It is initially unexpected that this reaction did not appear to occur because the $TiB_2$ reaction is known to be extremely violent [4]; however it is likely that this reaction did not initiate due to its size, as it has been shown that small diameter specimens of $TiB_2$ precursors do not initiate due to radial heat losses [6].

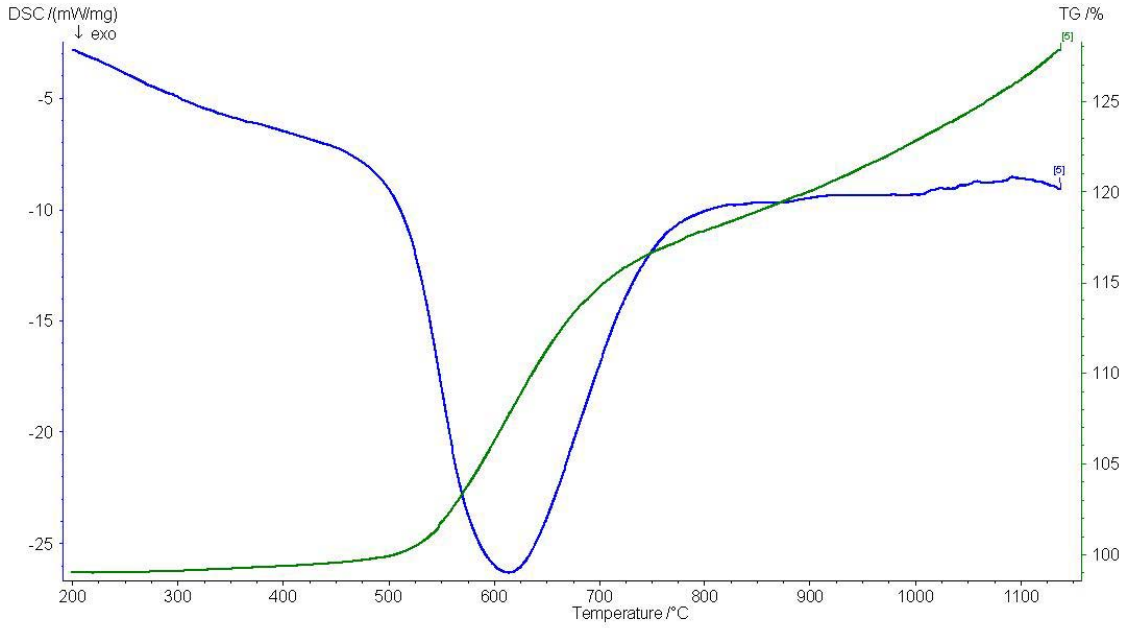


Figure 12: DSC and TG curves for $TiB_2$ formulated from 46µm Ti and 0.34µm B reacted in air. The exotherm beginning at approximately 500˚C corresponds to the boron DSC response. It does not appear that a reaction occurred.

### 3.2.2 Composite Blends

#### 3.2.2.1 Ignition Experiments

Figure 13 is a DSC curve for Ti-50Al + 40V% $TiB_2$ from which several characteristic values for this reaction system can be extracted. It is important to understand which of these values can and should be compared to the theoretical values of $T_{ig}$, $\Delta H_f$, and $T_{Ad}$. Due to the nature of the DSC measurements, the maximum temperature of reaction cannot be characterized in this instrument. Therefore the two-color infrared pyrometer was used as described previously. That leaves $T_{ig}$ and $\Delta H_f$ to be characterized using the DSC. There are three distinct features in Figure 13, those being an endotherm and two exotherms. In Figure 14 the curves for elemental titanium, aluminum, and boron are overlaid to aid in the comparison of the composite blend to its constituents. It should be noted that the DSC units are in mW/mg and that each of these specimens were approximately the same size, therefore the magnitude of the elemental constituents is inflated when compared to the composite blend. As such, only the location and relative magnitude of these peaks should be considered in the comparison.

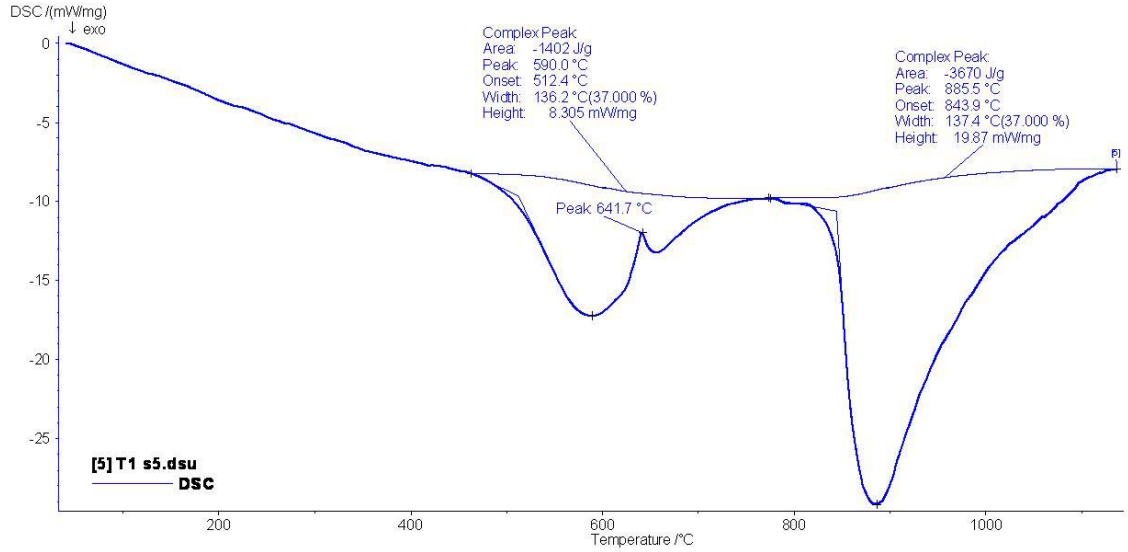


Figure 13: Representative DSC curve for the Ti-xAl + yV%$TiB_2$ reaction system. The exotherm beginning at approximately 450˚C is from boron, the endotherm at 641˚C is the melting endotherm of aluminum. The exotherm at approximately 850˚C could be from titanium or from the synthesis reaction.

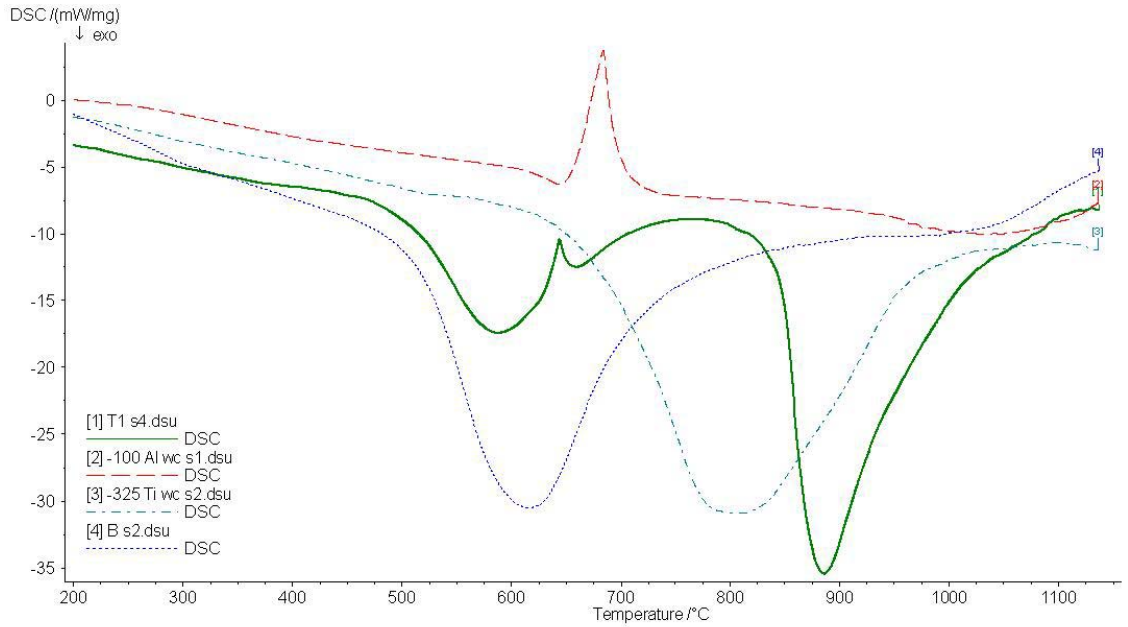


Figure 14: Representative DSC curve for the Ti-xAl + yV%$TiB_2$ reaction system with elemental titanium, aluminum, and boron curves. On the reaction curve we verify that the exotherm beginning at approximately 450˚C is from boron, the endotherm at 641˚C is the melting endotherm of aluminum. The exotherm at 850 is greater than the titanium exotherm and must therefore be as a result of the synthesis reaction.

The endotherm is the aluminum melting endotherm, the peak of it being taken as the melting temperature of aluminum ($T_{m, Al}$). It should be noted that the observed peak in the composite blend is lower than that of the elemental aluminum. This can be accounted for by the fact that the endotherm is within a heat producing exotherm, and due to a lag in response time of the thermocouple within the DSC from heat transfer the temperature at which the aluminum melts appears lower than it actually is.

The first, smaller exotherm could be an initial reaction; however when it is compared to the DSC curves from the three elemental constituents in Figure 14 the location of the exotherm matches that of the amorphous boron curve. Therefore, the specimen still appears to be a mixture of elemental titanium, aluminum and boron through the first exotherm.

The second exotherm appears larger than the first exotherm, and this is expected as the $aTi + bAl + cTi + dB \rightarrow zTiAl + yTiB_2$ reaction is known to be exothermic, therefore the area of that exotherm is taken to be the heat of reaction. To calculate the area of the exotherm the complex peak fit on the NETZSCH Proteus Thermal Analysis (Version 4.8.1) software was used. A procedure of maximizing the area term was used to ensure uniformity in the calculations. The resulting area value was taken to be $\Delta H_{rxn}$. The value was calculated by the software in units of J/g which were converted to units of kJ/mol by multiplying the value by the calculated theoretical atomic weight of the reacted composite and dividing by 1000.

Finally, the issue of ignition temperature remains. In the literature it has been assumed that ignition in the Ti-Al-B system occurs when the aluminum melts [11]. That does not appear to be the case presented in Figure 14. To determine if ignition occurs due to the aluminum melting, an experiment was designed to run under the same conditions as before, but with an isothermal hold at 750˚C for 20 minutes to see if the second reaction exotherm occurred. If the second exotherm appears then aluminum melting may be considered the ignition of the reaction. Figure 15 shows the results of this experiment. The secondary exotherm is not observed in this DSC curve. Another experiment was performed using the same profile as before with the addition of a 40 K/min ramp to 1150˚C following the 20 minute hold at 750˚C. The DSC curve for this experiment is shown in Figure 16. The second exotherm is observed in this case, and as

such indicates that the reaction is not initiated by the melting of aluminum, but rather requires more thermal energy to initiate. For the case of this report, the onset temperature calculated in the complex peak fit of the reaction exotherm is considered to be $T_{ig}$. It should be noted that similar to the suppression of the aluminum melting temperature this value may also be suppressed by the thermal lag within the instrument and as such it could be a source of error.

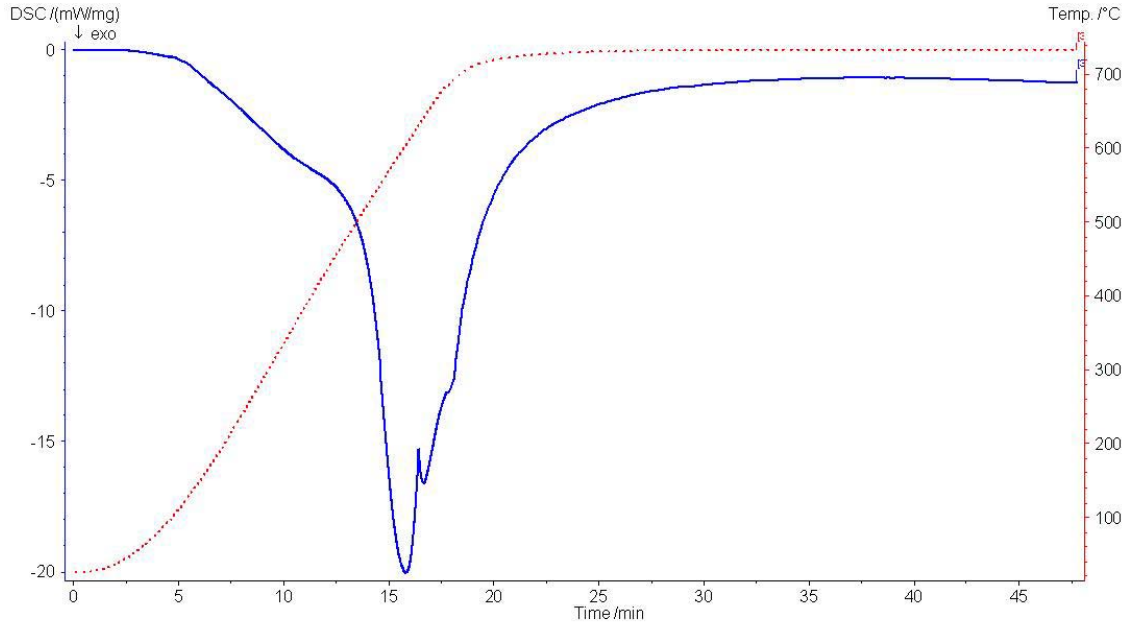


Figure 15: DSC curve for a Ti-50Al + 40V% $TiB_2$ reacted composition with an isothermal hold at 750˚C. The exotherm is from the boron and the endotherm is from aluminum. No exotherm appears during the isothermal hold, indicating that the reaction did not occur.

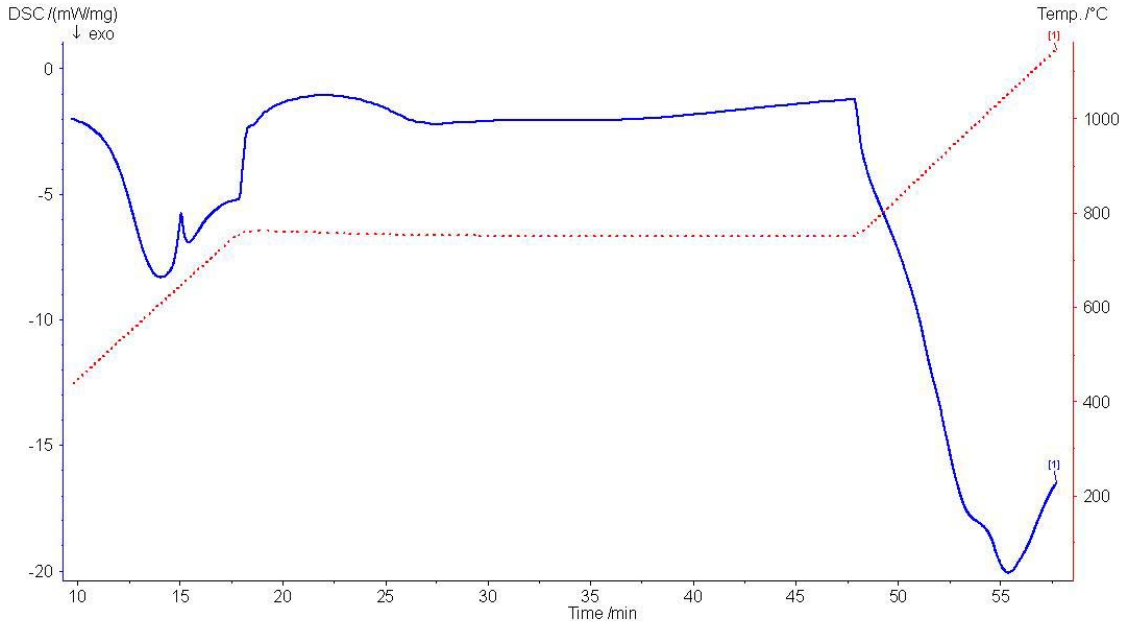


Figure 16: DSC curve for a Ti-50Al + 40V% $TiB_2$ reacted composition with an isothermal hold at 750˚C with a ramp to 1150˚C following the isothermal hold. The first exotherm is from the boron and the endotherm is from aluminum. Following the isothermal hold a second exotherm initiates, indicating that the reaction initiates above 750˚C.

A final note about the accuracy of the DSC measurements: the DSC is typically used to measure the energy that it puts into a material and the material's response, and it can measure these things accurately. In the case of these experiments, the reaction is extremely exothermic and occurs very rapidly. This leaves inherent issues of thermal lag and potential heat loss to the furnace environment which can and does affect measurement accuracy.

#### 3.2.2.2 Aluminide Content Experiments

Figure 17 shows the results for $T_{ig}$, and Table 9 shows its ANOVA table. The ANOVA shows, that at a 95% confidence level, that changing aluminum content does not affect the ignition temperature of the reaction. Therefore, the average $T_{ig}$ of all of these experiments was used in the theoretical calculations for the comparison of actual to theoretical.

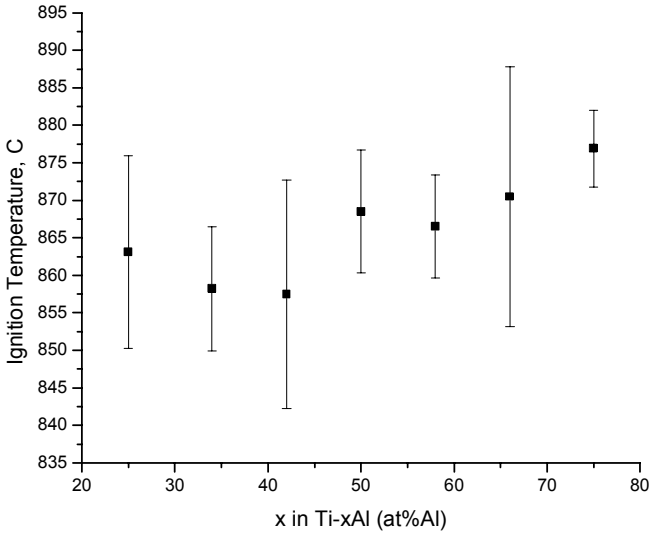


Figure 17: $T_{ig}$ results for varying at% Al in Ti-xAl + 40V% $TiB_2$ (error bars indicate one standard deviation).

| Dataset | N | Mean | Standard Deviation | Standard Error |
|---|---|---|---|---|
| Ti-25Al + 40V% $TiB_2$ | 3 | 863.07 | 12.84 | 7.41 |
| Ti-34Al + 40V% $TiB_2$ | 3 | 858.17 | 8.27 | 4.78 |
| Ti-42Al + 40V% $TiB_2$ | 2 | 857.45 | 15.20 | 10.75 |
| Ti-50Al + 40V% $TiB_2$ | 5 | 868.48 | 8.18 | 3.66 |
| Ti-58Al + 40V% $TiB_2$ | 3 | 866.53 | 6.89 | 3.98 |
| Ti-66Al + 40V% $TiB_2$ | 3 | 870.47 | 17.30 | 9.99 |
| Ti-75Al + 40V% $TiB_2$ | 3 | 876.93 | 5.14 | 2.97 |

| Source | DoF | SS | $SS_m$ | F Value | P Value |
|---|---|---|---|---|---|
| Model | 6 | 800.87 | 133.48 | 1.16968 | 0.37263 |
| Error | 15 | 1711.73 | 114.12 | | |

Table 9: ANOVA of $T_{ig}$ data.

Figure 18 shows the results of the $\Delta H_{rxn}$ data and the calculated $\Delta H_f$, and Table 10 is the corresponding ANOVA table. The ANOVA shows that varying the aluminum content in Ti-xAl + 40V% $TiB_2$ does have a significant affect on the exothermic heat of reaction. This affect follows the trend of the prediction, though the measured values are more exothermic than predicted. The measured values are more exothermic than the

theoretical calculations, possibly as a result of oxidation, or limitations associated with the measurement of the ignition temperature. The measured value of the $T_{ig}$ affects the calculated value of $\Delta H_f$.

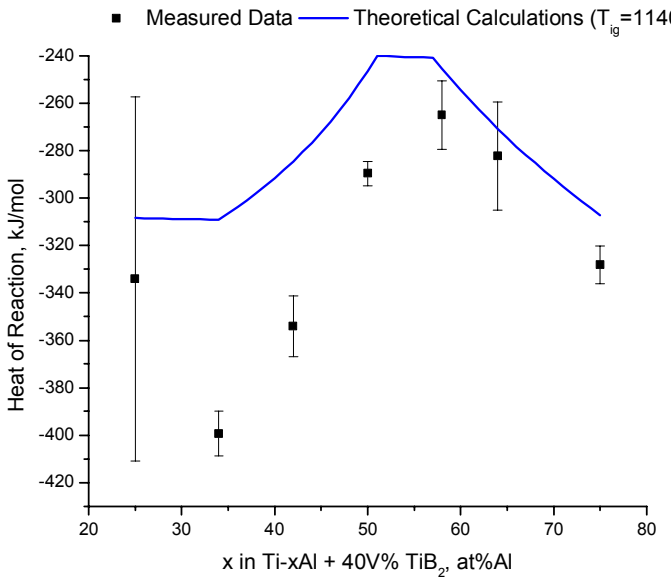


Figure 18: $\Delta H_{rxn}$ results for varying at% Al in Ti-xAl + 40V% $TiB_2$ with calculated $\Delta H_f$ values using $T_{ig}$ = 1140 K (error bars indicate one standard deviation).

| Dataset | N | Mean | Standard Deviation | Standard Error |
|---|---|---|---|---|
| Ti-25Al + 40V% $TiB_2$ | 3 | -334.07 | 76.77 | 44.32 |
| Ti-34Al + 40V% $TiB_2$ | 3 | -399.33 | 9.53 | 5.50 |
| Ti-42Al + 40V% $TiB_2$ | 2 | -354.15 | 12.80 | 9.05 |
| Ti-50Al + 40V% $TiB_2$ | 5 | -289.72 | 5.00 | 2.23 |
| Ti-58Al + 40V% $TiB_2$ | 3 | -264.97 | 14.55 | 8.40 |
| Ti-66Al + 40V% $TiB_2$ | 3 | -282.27 | 22.88 | 13.21 |
| Ti-75Al + 40V% $TiB_2$ | 3 | -328.13 | 7.94 | 4.59 |

| Source | DoF | SS | $SS_m$ | F Value | P Value |
|---|---|---|---|---|---|
| Model | 6 | 39801 | 6633.50 | 7.19561 | 0.00093 |
| Error | 15 | 13828.20 | 921.88 | | |

Table 10: ANOVA for $\Delta H_{rxn}$ data.

Figure 19 presents the results for $T_{max}$ and the calculated adiabatic temperature. The ANOVA of this data is shown in Table 11. The ANOVA indicated that at a 95%

confidence level the aluminum content has no affect on $T_{max}$ as is expected by the calculated values of $T_{Ad}$. The measured values for $T_{max}$ are lower than $T_{Ad}$ which is expected due to the limitations of the equipment and experimental set-up. Also, the calculations for $T_{Ad}$ are based on the assumption that the conditions upon reaction are adiabatic, meaning that the calculations assume no heat loss in the system. Though not easily quantifiable, it is certain that a specimen in a furnace open to room temperature air does experience heat loss, thus lowering the maximum temperature achieved during the reaction.

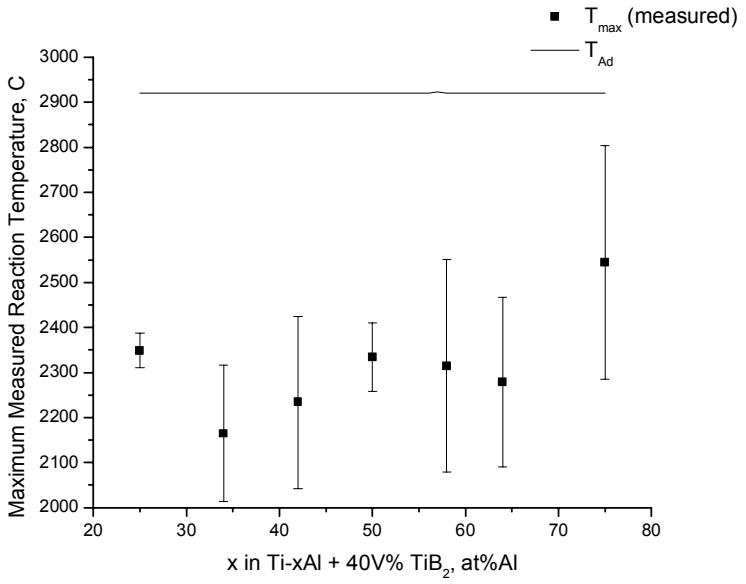


Figure 19: $T_{max}$ results for varying at% Al in Ti-xAl + 40V% $TiB_2$ (error bars indicate one standard deviation).

| Dataset | N | Mean | Standard Deviation | Standard Error |
|---|---|---|---|---|
| Ti-25Al + 40V% $TiB_2$ | 3 | 2348 | 38 | 22 |
| Ti-34Al + 40V% $TiB_2$ | 3 | 2164 | 151 | 87 |
| Ti-42Al + 40V% $TiB_2$ | 3 | 2234 | 191 | 110 |
| Ti-50Al + 40V% $TiB_2$ | 5 | 2335 | 76 | 34 |
| Ti-58Al + 40V% $TiB_2$ | 3 | 2315 | 236 | 136 |
| Ti-66Al + 40V% $TiB_2$ | 3 | 2278 | 188 | 109 |
| Ti-75Al + 40V% $TiB_2$ | 3 | 2544 | 259 | 150 |

| Source | DoF | SS | $SS_m$ | F Value | P Value |
|---|---|---|---|---|---|
| Model | 6 | 254575 | 42429 | 1.46994 | 0.2502 |
| Error | 16 | 461835 | 28865 | | |

Table 11: ANOVA for $T_{max}$ data.

## 3.3 Extrinsic Reactant Variables

Extrinsic reactant variables are expected to affect the behavior of the reaction. The affect cannot be directly upon the values of $\Delta H_{rxn}$ and $T_{max}$ as they are values that are, or are calculated from, state thermodynamic values. However, $T_{ig}$ is not a thermodynamic value, but is highly influenced by kinetics. Therefore, the only reaction behavior that should be affected is $T_{ig}$, which will affect $\Delta H_{rxn}$ and $T_{max}$ because they are dependent upon the value of $T_{ig}$. From the enthalpy loop plots such as that shown in Figure 4, we expect that increasing $T_{ig}$ would decrease $\Delta H_{rxn}$ and increase $T_{max}$.

The results from the Taguchi L4 array conducted on the Ti-50Al + 20V%$TiB_2$ and Ti-50Al + 40V%$TiB_2$ composite blends are presented in Sections 3.3.1 and 3.3.2 respectively. The reason for conducting this experiment with two different volume percentages of $TiB_2$, is to determine if there is a difference in response resulting from changing the reinforcement percentage.

### 3.3.1 Ti-50Al + 20V% $TiB_2$

The results of the two-way ANOVA on the ignition temperature of the reaction are shown in Table 12. At the 95% confidence level it shows that the aluminum particle

size, titanium particle size, and the interaction of aluminum and titanium particle size are significant.

| Source | DoF | SS | $SS_m$ | F Value | P Value |
|---|---|---|---|---|---|
| Aluminum Particle Size | 1 | 1875.98 | 1875.98 | 20.9515 | 0.00031 |
| Titanium Particle Size | 1 | 7940.11 | 7940.11 | 88.6775 | 0 |
| Al size × Ti size | 1 | 3157.58 | 3157.58 | 35.2648 | 0.00002 |
| Error | 16 | 1432.63 | 89.54 | | |

Table 12: Two-way ANOVA results for $T_{ig}$ of Ti-50Al + 20V% $TiB_2$.

Figure 20 shows the average $T_{ig}$ at different aluminum, and titanium particle sizes, along with the interaction plot of aluminum and titanium particle size. The coarser aluminum particles appear increase $T_{ig}$ and the coarser titanium particle size causes the reaction to have a lower ignition temperature. The interaction plot in part c) shows an interaction. Increasing the aluminum particle size in the blends with 99µm titanium dramatically increases the ignition temperature, where in the blends with 46µm titanium the larger particle size of the aluminum decreases the ignition temperature slightly.

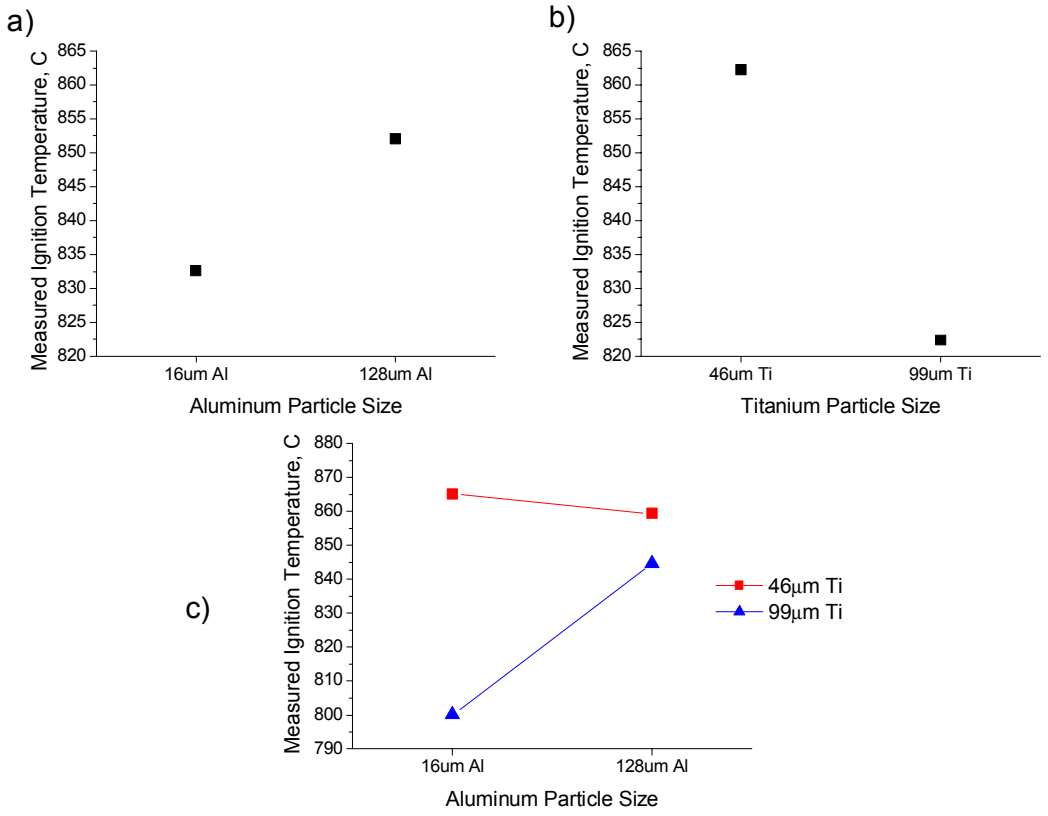


Figure 20: The average values of $T_{ig}$ in the Ti-50Al + 20V% $TiB_2$ reaction for a) different aluminum particle sizes, b) different titanium particle sizes, and c) the interaction of aluminum and titanium particle sizes.

Table 13 shows the results of the two-way ANOVA on $\Delta H_{rxn}$. It shows that at the 95% confidence level only the titanium particle size is significant.

| Source | DoF | SS | $SS_m$ | F Value | P Value |
|---|---|---|---|---|---|
| Aluminum Particle Size | 1 | 46677.20 | 46677.20 | 3.85136 | 0.06734 |
| Titanium Particle Size | 1 | 57104.50 | 57104.50 | 4.71173 | 0.04535 |
| Al size × Ti size | 1 | 21522.91 | 21522.91 | 1.77587 | 0.20133 |
| Error | 16 | 193914.47 | 12119.65 | | |

Table 13: Two-way ANOVA results for $\Delta H_{rxn}$ of Ti-50Al + 20V% $TiB_2$.

Figure 21 shows the plot of $\Delta H_{rxn}$ at the different aluminum and titanium particle sizes, along with the interaction plot of aluminum and titanium particle size. The aluminum particle size appears to have no effect. The finer titanium particle size results

in more exothermic heat of reaction. This is the opposite of what the expected affect on $\Delta H_{rxn}$ is from the observed affects on $T_{ig}$. Therefore, there are most likely some other extrinsic affects that are causing this variation. The interaction plot shows the possibility of an interaction; however the calculated P Value for the interaction shows that it is not significant at the 95% confidence level.

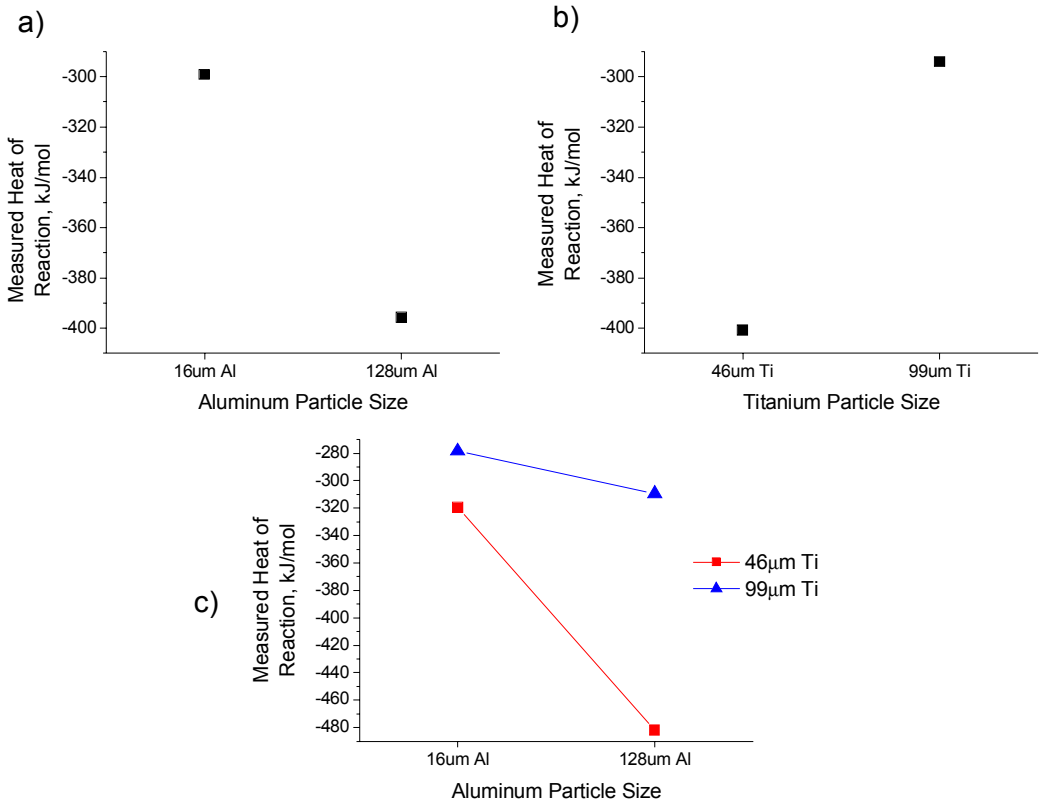


Figure 21: The average values of $\Delta H_{rxn}$ in the Ti-50Al + 20V% $TiB_2$ reaction for a) different aluminum particle sizes, b) different titanium particle sizes, and c) the interaction of aluminum and titanium particle sizes.

Table 14 shows the two-way ANOVA on $T_{max}$. It shows that at the 95% confidence level that the titanium particle size is significant.

| Source | DoF | SS | $SS_m$ | F Value | P Value |
|---|---|---|---|---|---|
| Aluminum Particle Size | 1 | 1201.25 | 1201.25 | 0.22707 | 0.64015 |
| Titanium Particle Size | 1 | 110558.45 | 110558.45 | 20.8988 | 0.00031 |
| Al size × Ti size | 1 | 2142.45 | 2142.45 | 0.40499 | 0.53352 |
| Error | 16 | 84642.80 | 5290.18 | | |

Table 14: Two-way ANOVA results for $T_{max}$ of Ti-50Al + 20V% $TiB_2$.

Figure 22 shows the plot of $T_{max}$ at the different aluminum and titanium particle sizes, along with the interaction plot of aluminum and titanium particle size. The aluminum particle size appears to have no effect, while the coarser titanium powder yielded a higher maximum temperature than the finer titanium powder. Again, this is contrary to what would be expected from the affect of particle size on $T_{ig}$, and thus $T_{ig}$ on $T_{max}$. The interaction plot shows no real possibility of an interaction.

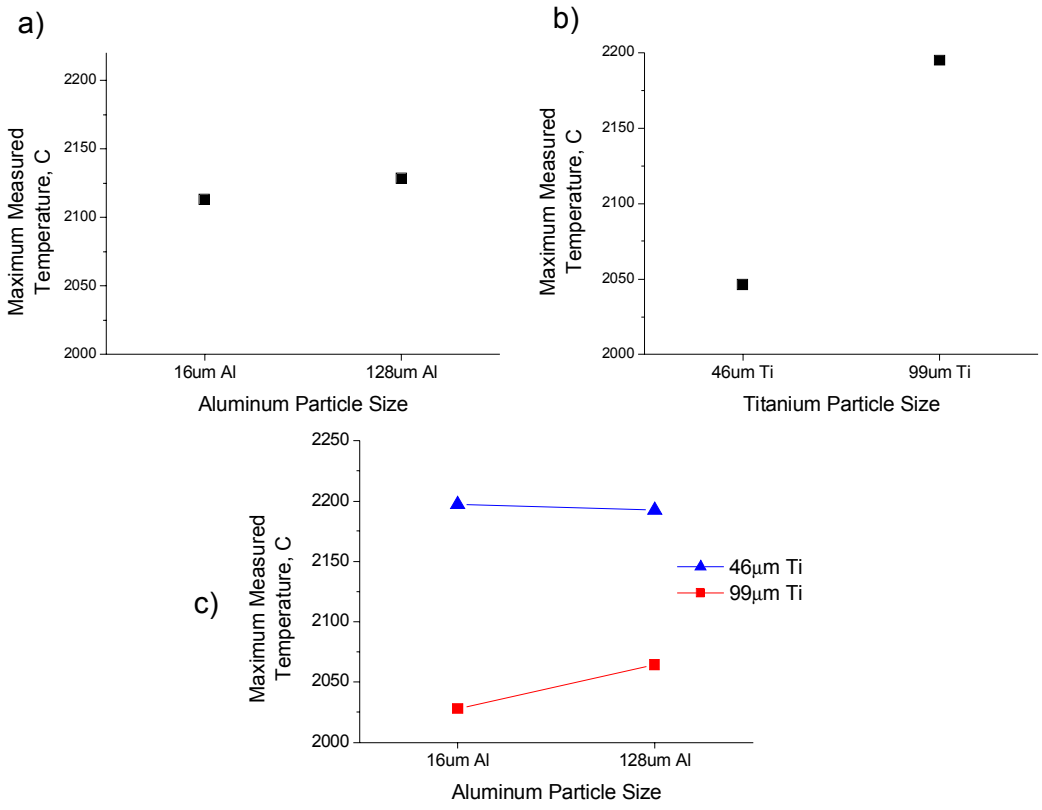


Figure 22: The average values of $T_{max}$ in the Ti-50Al + 20V% $TiB_2$ reaction for a) different aluminum particle sizes, b) different titanium particle sizes, and c) the interaction of aluminum and titanium particle sizes.

### 3.3.2 Ti-50Al + 40V% $TiB_2$

Table 15 shows the two-way ANOVA results for $T_{ig}$. The analysis reveals that at the 95% confidence level that aluminum and titanium particle size are significant.

| Source | DoF | SS | $SS_m$ | F Value | P Value |
|---|---|---|---|---|---|
| Aluminum Particle Size | 1 | 3117.50 | 3117.50 | 17.0242 | 0.00079 |
| Titanium Particle Size | 1 | 3861.42 | 3861.42 | 21.0866 | 0.0003 |
| Al size × Ti size | 1 | 209.30 | 209.30 | 1.14298 | 0.30089 |
| Error | 16 | 2929.96 | 183.12 | | |

Table 15: Two-way ANOVA results for $T_{ig}$ of Ti-50Al + 40V% $TiB_2$.

Figure 23 shows the average $T_{ig}$ at different aluminum, and titanium particle sizes, along with the interaction plot of aluminum and titanium particle size. The coarser aluminum particles appear increase $T_{ig}$ and the coarser titanium particle size causes the reaction to have a lower ignition temperature. No interaction is apparent from part c) as the lines in the interaction plot are close to parallel.

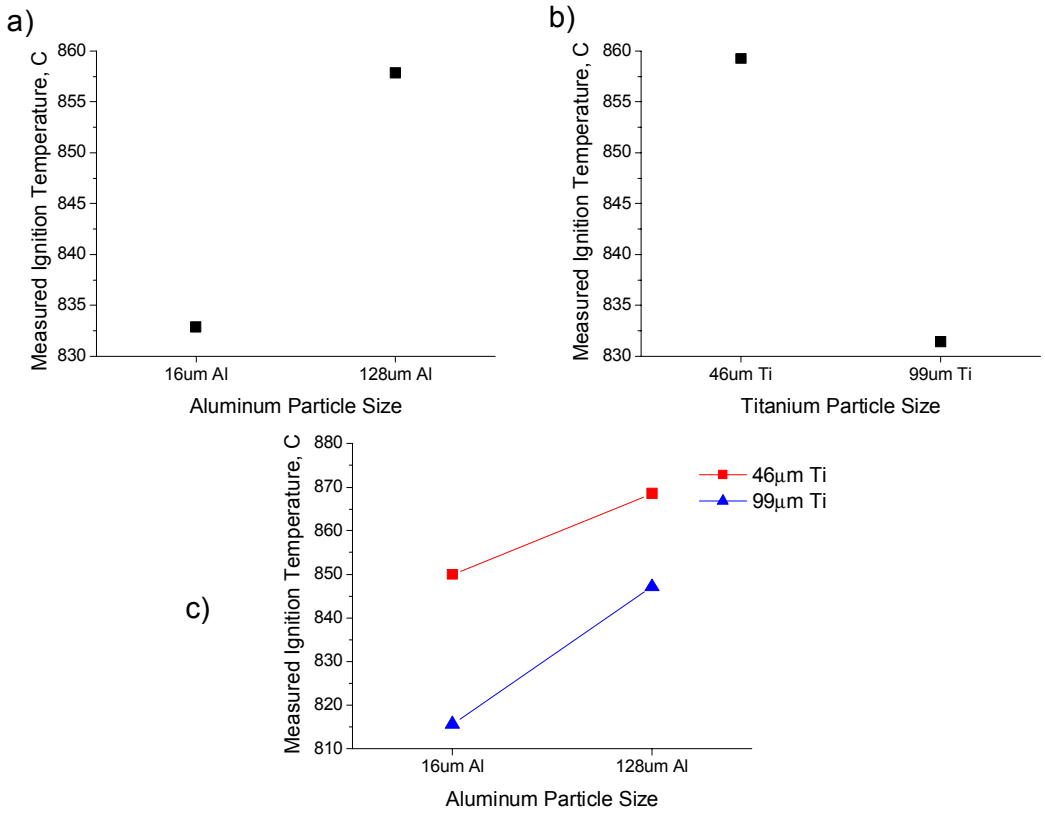


Figure 23: The average values of $T_{ig}$ in the Ti-50Al + 40V% $TiB_2$ reaction for a) different aluminum particle sizes, b) different titanium particle sizes, and c) the interaction of aluminum and titanium particle sizes.

Table 16 shows the results of the two-way ANOVA on $\Delta H_{rxn}$. The analysis shows that only titanium particle size is significant at the 95% confidence level.

| Source | DoF | SS | $SS_m$ | F Value | P Value |
|---|---|---|---|---|---|
| Aluminum Particle Size | 1 | 585.33 | 585.33 | 0.35623 | 0.55896 |
| Titanium Particle Size | 1 | 43313.76 | 43313.76 | 26.3605 | 0.0001 |
| Al size × Ti size | 1 | 6925.14 | 6925.14 | 4.21459 | 0.0568 |
| Error | 16 | 26290.14 | 1643.13 | | |

Table 16: Two-way ANOVA results for $\Delta H_{rxn}$ of Ti-50Al + 40V% $TiB_2$.

Figure 24 shows the plot of $\Delta H_{rxn}$ at the different aluminum and titanium particle sizes, along with the interaction plot of aluminum and titanium particle size. The aluminum particle size appears to have no effect. The finer titanium particle size results in more exothermic heat of reaction. Similarly to the Ti-50Al + 20V% $TiB_2$ results this is

contrary to what would be expected from the affect of the particle size on $T_{ig}$, and thus $\Delta H_{rxn}$. The interaction plot shows the possibility of an interaction; however the calculated P Value for the interaction in Table 16 shows that it is not significant at the 95% confidence level though it is close.

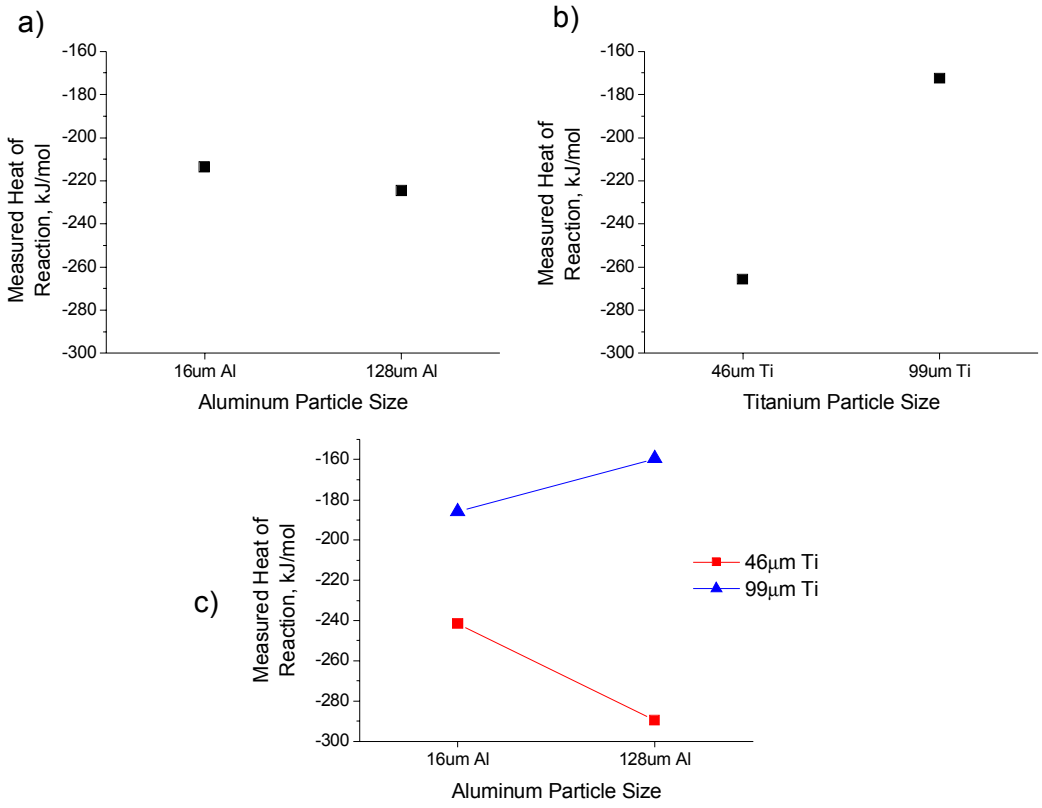


Figure 24: The average values of $\Delta H_{rxn}$ in the Ti-50Al + 40V% $TiB_2$ reaction for a) different aluminum particle sizes, b) different titanium particle sizes, and c) the interaction of aluminum and titanium particle sizes.

The two-way ANOVA of $T_{max}$ is shown in Table 17. The analysis shows that the titanium particle size is significant at the 95% confidence level.

| Source | DoF | SS | $SS_m$ | F Value | P Value |
|---|---|---|---|---|---|
| Aluminum Particle Size | 1 | 4560.20 | 4560.20 | 0.68378 | 0.42045 |
| Titanium Particle Size | 1 | 89244.80 | 89244.80 | 13.3818 | 0.00212 |
| Al size × Ti size | 1 | 4440.20 | 4440.20 | 0.66579 | 0.42651 |
| Error | 16 | 106705.60 | 6669.10 | | |

Table 17: Two-way ANOVA results for $T_{max}$ of Ti-50Al + 40V% $TiB_2$.

Figure 25 shows the plot of $T_{max}$ at the different aluminum and titanium particle sizes, along with the interaction plot of aluminum and titanium particle size. The aluminum particle size appears to have no effect. The coarser titanium particle size results in a higher $T_{max}$, which is contrary to what would be expected from the observed effects on $T_{ig}$. The interaction plot shows no real possibility of an interaction.

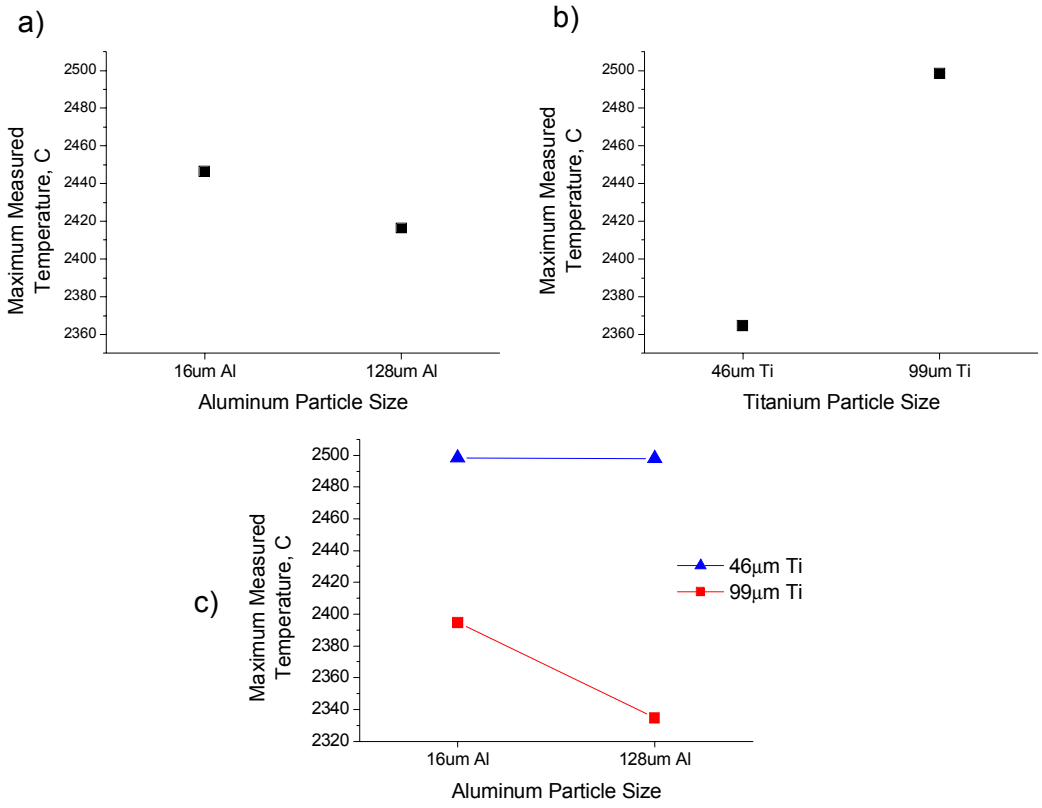


Figure 25: The average values of $T_{max}$ in the Ti-50Al + 40V% $TiB_2$ reaction for a) different aluminum particle sizes, b) different titanium particle sizes, and c) the interaction of aluminum and titanium particle sizes.

In summary, in both the Ti-50Al + 20V% $TiB_2$ and Ti-50Al + 40V% $TiB_2$ composite blends the titanium particle size was shown to have an effect on the behavior of the synthesis reaction. The measured affect on $\Delta H_{rxn}$ and $T_{max}$ was opposite of what would be expected from the measured affect on $T_{ig}$. Thus, it is likely that some other extrinsic variable(s) are causing this difference between the measured and predicted affect on $\Delta H_{rxn}$ and $T_{max}$.

# 4 Conclusions

This project was a study of the effects of changing the formulation and extrinsic reaction variables on the reaction behavior of the Ti-xAl + yV% $TiB_2$ reaction system. A program was successfully created to perform the needed calculations to theoretically predict the reaction behavior of the composite reaction system. Results based upon published thermodynamic data indicated a minimal effect of matrix stoichiometry and strong effect of reinforcement percentage on $T_{Ad}$, and a strong effect of matrix stoichiometry and reinforcement percentage on $\Delta H_f$.

In the process of determining the ignition temperature in the Ti-xAl + 40V% $TiB_2$ reaction system it was shown that the initiation of this reaction is not from the melting of the aluminum metal, but that the reaction ignites at a temperature higher than that showing that more thermal energy is required to overcome the kinetic limitations on the reaction. Since the ignition temperature, as determined from the DSC results, was not significantly different for the different matrix compositions we can infer that the ignition mechanism is consistent in the Ti-Al-B reaction system.

Measurements from high-speed pyrometry indicated that $T_{max}$ varied little with matrix stoichiometry, and were also lower than the predictions ($T_{max} \approx 0.8\ T_{Ad}$).

Measurements from DSC indicated that $T_{ig}$ is independent of matrix stoichiometry and that $\Delta H_{rxn}$ follows the predicted trend, though is more exothermic than predicted.

Finally, the particle sizes of the titanium and aluminum powders were shown to have an effect on the behavior of the synthesis reaction. The observed effects of the particle size on $\Delta H_{rxn}$ and $T_{max}$ do not match what would be expected from its effects on $T_{ig}$ indicating that other extrinsic variables may be affecting the behavior of the reaction.

# 5 Future Work

The program is quite useful in predicting the behavior of the Ti-xAl + yV% $TiB_2$ system, however some major assumptions were made in the building of the program. The accuracy of the program would be benefit from having actual H(T) data for $Ti_3Al$. Incorporating oxidation into the program would be useful, as it is likely that oxidation could significantly change the behavior of $T_{Ad}$ and $\Delta H_f$. Incorporating oxidation into the predictions could aide in determining if the observed difference between $\Delta H_{rxn}$ and $\Delta H_f$ is a result of oxidation or due to limitations associated with the measurement. Finally, incorporating a function to calculate the phase boundaries as a function of $T_{ig}$ would also increase the program's accuracy.

The theoretical calculations are all dependent on $T_{ig}$, therefore it would be useful to gain an understanding of the mechanism of ignition and how formulation and extrinsic factors affect the ignition temperature. Also, since there was no direct measurement of $T_{ig}$ in this study, it would be useful to measure the temperature of the material throughout the heating profile to have an accurate value of $T_{ig}$ for use in the theoretical calculations.

Evaluating the effects of varying the aluminide content in composite systems with less $TiB_2$ in the reacted composite would be useful to see if the effects are similar across a wide range of reinforcement percentages.

Characterization of reacted material would provide the actual composition of the composite. This would provide a check for the composition assumptions in the calculations, allowing for program modifications to more accurately represent the actual system.

# 6 Appendix A: Thermochemical Data

A summary of the enthalpy data (kJ/mol) used for adiabatic temperature and heat of formation calculations for Ti-xAl plus $TiB_2$ particulate composites [12]

| | T, K | Al | Ti | Amorphous Boron | Crystalline Boron | TiAl | $Al_3Ti$ | $TiAl_3$ | $TiB_2$ |
|---|---|---|---|---|---|---|---|---|---|
| | 298.00 | 0.00 | 0.00 | 48.93 | 0.00 | -75.31 | -146.44 | -146.44 | -323.80 |
| | 300.00 | 0.05 | 0.05 | 48.95 | 0.02 | -75.31 | -146.26 | -146.26 | -323.72 |
| | 400.00 | 2.55 | 2.64 | 50.31 | 1.39 | -70.05 | -136.02 | -136.02 | -318.67 |
| | 500.00 | 5.19 | 5.34 | 52.04 | 3.12 | -64.56 | -125.32 | -125.32 | -312.81 |
| | 600.00 | 7.95 | 8.12 | 54.02 | 5.10 | -58.89 | -114.29 | -114.29 | -306.44 |
| | 700.00 | 10.82 | 10.99 | 56.18 | 7.25 | -53.09 | -103.02 | -103.02 | -299.67 |
| | 800.00 | 13.82 | 13.96 | 58.46 | 9.54 | -47.19 | -91.52 | -91.52 | -292.60 |
| | 900.00 | 17.01 | 17.05 | 60.84 | 11.92 | -41.19 | -79.52 | -79.52 | -285.25 |
| $T_{mp}$ of Al | 933.45 | 18.13 | 0 | 0 | 0 | 0 | 0 | 0 | 0 |
| | 933.45 | 28.84 | 0 | 0 | 0 | 0 | 0 | 0 | 0 |
| | 1000.00 | 30.95 | 20.24 | 63.30 | 14.38 | -35.12 | -67.93 | -67.93 | -277.65 |
| | 1100.00 | 34.13 | 23.55 | 65.83 | 16.91 | -28.97 | -55.85 | -55.85 | -269.82 |
| $\alpha$ - $\beta$ for Ti | 1166.00 | 0 | 25.78 | 0 | 0 | 0 | 0 | 0 | 0 |
| | 1166.00 | 0 | 29.95 | 0 | 0 | 0 | 0 | 0 | 0 |
| | 1200.00 | 37.30 | 30.96 | 68.42 | 19.50 | -22.75 | -43.60 | -43.60 | -261.79 |
| | 1300.00 | 40.47 | 33.94 | 71.06 | 22.14 | -16.46 | -31.16 | -31.16 | -253.55 |
| | 1400.00 | 43.65 | 36.99 | 73.75 | 24.83 | -10.10 | -18.55 | -18.55 | -245.13 |
| | 1500.00 | 46.82 | 40.11 | 76.49 | 27.56 | -3.68 | -5.76 | -5.76 | -236.53 |
| | 1600.00 | 50.00 | 43.30 | 79.26 | 30.34 | 2.80 | 7.19 | 7.19 | -227.76 |
| $T_{mp}$ of $Al_3Ti$ | 1613.00 | 0 | 0 | 0 | 0 | 0 | 8.86 | 8.86 | 0 |
| | 1613.00 | 0 | 0 | 0 | 0 | 0 | 88.86 | 88.86 | 0 |
| | 1700.00 | 53.16 | 46.58 | 82.08 | 33.16 | 9.35 | 100.18 | 100.18 | -218.83 |
| $T_{mp}$ of TiAl | 1733.00 | 0 | 0 | 0 | 0 | 11.52 | 0 | 0 | 0 |
| | 1733.00 | 0 | 0 | 0 | 0 | 71.52 | 0 | 0 | 0 |
| | 1800.00 | 56.35 | 49.95 | 84.94 | 36.01 | 75.97 | 113.20 | 113.20 | -209.75 |
| | 1900.00 | 59.52 | 53.41 | 87.83 | 38.90 | 82.61 | 126.22 | 126.22 | -200.53 |
| $T_{mp}$ of Ti | 1939.00 | 0 | 54.79 | 0 | 0 | 0 | 0 | 0 | 0 |
| | 1939.00 | 0 | 68.93 | 0 | 0 | 0 | 0 | 0 | 0 |
| | 2000.00 | 62.70 | 71.10 | 90.76 | 41.83 | 89.24 | 139.24 | 139.24 | -191.17 |
| | 2100.00 | 65.87 | 74.66 | 93.72 | 44.79 | 95.88 | 152.26 | 152.26 | -181.68 |
| | 2200.00 | 69.05 | 78.22 | 96.72 | 47.79 | 102.52 | 165.27 | 165.27 | -172.06 |
| | 2300.00 | 72.22 | 81.77 | 99.75 | 50.82 | 109.16 | 178.29 | 178.29 | -162.34 |
| $T_{mp}$ of $\beta$-B | 2350.00 | 0 | 0 | 0 | 52.34 | 0 | 0 | 0 | 0 |
| | 2350.00 | 0 | 0 | 0 | 101.26 | 0 | 0 | 0 | 0 |
| | 2400.00 | 75.40 | 85.33 | 104.14 | 104.14 | 115.80 | 191.31 | 191.31 | -152.50 |
| | 2500.00 | 78.57 | 88.89 | 107.32 | 107.32 | 122.43 | 204.33 | 204.33 | -142.57 |
| | 2600.00 | 81.75 | 92.44 | 110.49 | 110.49 | 129.07 | 217.35 | 217.35 | -132.54 |
| | 2700.00 | 84.92 | 96.00 | 113.67 | 113.67 | 135.71 | 230.36 | 230.36 | -122.43 |
| $T_{vap}$ of Al | 2790.81 | 87.52 | 0 | 0 | 0 | 0 | 0 | 0 | 0 |
| | 2790.81 | 381.60 | 0 | 0 | 0 | 0 | 0 | 0 | 0 |

| | | | | | | | | | |
|---|---|---|---|---|---|---|---|---|---|
| | 2800.00 | 381.86 | 99.56 | 116.84 | 116.84 | 142.35 | 243.38 | 243.38 | -112.23 |
| | 2900.00 | 383.94 | 103.11 | 120.02 | 120.02 | 148.99 | 256.40 | 256.40 | -101.97 |
| | 3000.00 | 386.01 | 106.67 | 123.19 | 123.19 | 155.62 | 269.42 | 269.42 | -91.63 |
| | 3100.00 | 388.09 | 110.22 | 126.37 | 126.37 | 162.26 | 282.44 | 282.44 | -81.24 |
| $T_{mp}$ of $TiB_2$ | 3193.00 | 0 | 0 | 0 | 0 | 0 | 0 | 0 | -71.53 |
| | 3193.00 | 0 | 0 | 0 | 0 | 0 | 0 | 0 | 28.89 |
| | 3200.00 | 390.17 | 113.78 | 129.54 | 129.54 | 168.90 | 295.45 | 295.45 | 29.65 |
| | 3300.00 | 392.25 | 117.34 | 132.72 | 132.72 | 175.54 | 308.47 | 308.47 | 40.53 |
| | 3400.00 | 394.33 | 120.89 | 135.89 | 135.89 | 182.18 | 321.49 | 321.49 | 51.40 |
| | 3500.00 | 396.41 | 124.45 | 139.07 | 139.07 | 188.81 | 334.51 | 334.51 | 62.28 |

# 7 Appendix B: Matlab Program Code

**MainTiAlTiB2.m**

```
% This program is written for the Ti-XAl + V%TiB2 MMC system

clear
close all
clc

fprintf('Select desired output:\n');
fprintf('1 - Enthalpy loop plot, Adiabatic Temperature, and Heat of Reaction for a given
matrix composition\n');
fprintf('2 - Adiabatic Temperature vs. Volume Percent of TiB2 for a given matrix
composition\n');
fprintf('3 - Atomic weight for a given composite formulation\n');
fprintf('4 - Adiabatic Temperature and Heat of Formation vs. percent Al for a given
amount of TiB2\n');
fprintf('5 - Atomic percentages of Ti3Al, TiAl, and TiAl3 in Ti-xAl\n')
type = input('Enter Choice --> ');

if type == 1
   fprintf('Input Desired Fraction of Aluminum in the Matrix (i.e. Ti-XAl)\n');
   fprintf('(This will be between 25 and 75)\n');
   X_Al = input('X_Al --> ');
   fprintf('Input Desired Volume Fraction of TiB2\n');
   fprintf('(This will be between 0 and 100)\n');
   Vper_TiB2 = input('V% TiB2 --> ');

   yesno = input('Do you want to input an ignition temperature (1 - for yes, 2 - for no
(uses 1000K))\n');
   if yesno == 1
      fprintf('Enter the Ignition Temperature (K)\n');
      T_ig = input('T_ig --> ');
   else
      T_ig = 1000;
   end

   % Puts the inputs into fraction form
   X_Al = X_Al/100;
   X_Ti = 1 - X_Al;
   Vper_TiB2 = Vper_TiB2/100;

   % Calls EnthalpyCalc2 Function, which calculates the enthalpies of the matrix -
Enthalpy loops
```

```
   [T_Adiabatic,DHrxn] = EnthalpyCalc2(X_Al,Vper_TiB2,T_ig);
   fprintf('T_Adiabatic (K) = %g',T_Adiabatic)
   fprintf('\n')
   fprintf('DHrxn (kJ/mol) = %g',DHrxn)

end

if type == 2
   fprintf('Input Desired Fraction of Aluminum in the Matrix (i.e. Ti-XAl)\n');
   fprintf('(This will be between 25 and 75)\n');
   X_Al = input('X_Al --> ');

   yesno = input('Do you want to input an ignition temperature (1 - for yes, 2 - for no
(uses 1000K))\n');
   if yesno == 1
      fprintf('Enter the Ignition Temperature (K)\n');
      T_ig = input('T_ig --> ');
   else
      T_ig = 1000;
   end

   % Puts the inputs into fraction form
   X_Al = X_Al/100;
   X_Ti = 1 - X_Al;

   % Calls AdiabaticCalc Function, which calculates the Adiabatic Temperature vs.
V%TiB2 plot
   [Vper_TiB2_plot,T_ad_plot] = AdiabaticCalc(X_Al,T_ig);
end

if type == 3
   fprintf('Input Desired Fraction of Aluminum in the Matrix (i.e. Ti-XAl)\n');
   fprintf('(This will be between 25 and 75)\n');
   X_Al = input('X_Al --> ');
   fprintf('Input Desired Volume Fraction of TiB2\n');
   fprintf('(This will be between 0 and 100)\n');
   Vper_TiB2 = input('V% TiB2 --> ');

   % Puts the inputs into fraction form
   Vper_TiB2 = Vper_TiB2/100;
   X_Al = X_Al / 100;
   X_Ti = 1 - X_Al;
   % Calls AluminideCalc Function, which calculates the atomic weight and density of
the matrix
   [AW_TiXAl,d_TiXAl] = AluminideCalc(X_Al,X_Ti);
```

```
   % Calls CompositionCalc Function, which calculates the atomic percentages of the
matrix and reinforcement in the composite
   [atper_TiXAl,atper_TiB2,AW_composite] =
CompositionCalc(AW_TiXAl,d_TiXAl,Vper_TiB2,X_Al,X_Ti);
   fprintf('AW_composite (g/mole) = %g',AW_composite);
end

if type == 4
   fprintf('Input Desired Volume Fraction of TiB2\n');
   fprintf('(This will be between 0 and 100)\n');
   Vper_TiB2 = input('V% TiB2 --> ');

   yesno = input('Do you want to input an ignition temperature (1 - for yes, 2 - for no
(uses 1000K))\n');
   if yesno == 1
      fprintf('Enter the Ignition Temperature (K)\n');
      T_ig = input('T_ig --> ');
   else
      T_ig = 1000;
   end

   % Puts the inputs into fraction form
   Vper_TiB2 = Vper_TiB2/100;

   % Calls TadHrxnAllXs Function, which calculated the TAd and DHrxn curves across
the aluminum range for a given V% TiB2
   [X_Al_plot,T_Ad_output,DHrxn_output] = TadHrxnAllXs(Vper_TiB2,T_ig);
end

if type == 5
   fprintf('Input Desired Fraction of Aluminum in the Matrix (i.e. Ti-XAl)\n');
   fprintf('(This will be between 25 and 75)\n');
   X_Al = input('X_Al --> ');

   % Puts the inputs into fraction form
   X_Al = X_Al / 100;
   X_Ti = 1 - X_Al;

   % Calls AluminideFrac Function, which calculates the fractions of each titanium
aluminide in the matrix
   [atper_Ti3Al,atper_TiAl,atper_Al3Ti] = AluminideFrac(X_Al,X_Ti);
   fprintf('atper Ti3Al = %g\n',atper_Ti3Al);
   fprintf('atper TiAl = %g\n',atper_TiAl);
   fprintf('atper Al3Ti = %g\n',atper_Al3Ti);
end
```

**AluminideFrac Subroutine**

```
   % Calls AluminideFrac Function, which calculates the fractions of each titanium
aluminide in the matrix
   [atper_Ti3Al,atper_TiAl,atper_Al3Ti] = AluminideFrac(X_Al,X_Ti);
   fprintf('atper Ti3Al = %g\n',atper_Ti3Al);
   fprintf('atper TiAl = %g\n',atper_TiAl);
   fprintf('atper Al3Ti = %g\n',atper_Al3Ti);
end
```

**AluminideCalc Subroutine**

```
function [AW_TiXAl,d_TiXAl] = AluminideCalc(X_Al,X_Ti)

% Densities and Atomic Weights of TiAl, Ti3Al, and Al3Ti
d_TiAl = 3.91;
AW_TiAl = 75.2;

d_Al3Ti = 3.4;
AW_Al3Ti = 128.84;

d_Ti3Al = 4.2;
AW_Ti3Al = 170.68;

[atper_Ti3Al,atper_TiAl,atper_Al3Ti] = AluminideFrac(X_Al,X_Ti);

AW_TiXAl = atper_Ti3Al * AW_Ti3Al + atper_TiAl * AW_TiAl + atper_Al3Ti *
AW_Al3Ti;
d_TiXAl = atper_Ti3Al * d_Ti3Al + atper_TiAl * d_TiAl + atper_Al3Ti * d_Al3Ti;
```

**CompositionCalc Subroutine**

```
function [atper_TiXAl,atper_TiB2,AW_composite] =
CompositionCalc(AW_TiXAl,d_TiXAl,Vper_TiB2,X_Al,X_Ti)

d_TiB2 = 4.50;
AW_TiB2 = 69.522;

Vper_TiXAl = 1 - Vper_TiB2;

n_TiXAl = Vper_TiXAl * d_TiXAl / AW_TiXAl;
n_TiB2 = Vper_TiB2 * d_TiB2 / AW_TiB2;
n_Total = n_TiXAl + n_TiB2;

atper_TiXAl = n_TiXAl / n_Total;
atper_TiB2 = n_TiB2 / n_Total;
```

```
AW_composite = atper_TiXAl * AW_TiXAl + atper_TiB2 * AW_TiB2;
```

**abcdCalc Subroutine**

```
function [a,b,c,d] = abcdCalc(X_Al,X_Ti,atper_TiXAl,atper_TiB2)

% Calculates the multipliers for Enthalpy Calculations (a*Ti + b*Al + c*Ti + d*B ->
atper_TiXAl*TiXAl + atper_TiB2*TiB2)

a = 2 * X_Ti * atper_TiXAl; % Multiplier for Matrix Titanium
b = 2 * X_Al * atper_TiXAl; % Multiplier for Matrix Aluminum
c = atper_TiB2;             % Multiplier for Reniforcement Titanium
d = 2 * atper_TiB2;         % Multiplier for Reinforcement Boron
```

**EnthalpyCalc2 Subroutine**

```
function [T_Adiabatic,DHrxn] = EnthalpyCalc2(X_Al,Vper_TiB2,T_ig)

X_Ti = 1 - X_Al;

% Calls AluminideCalc Function, which calculates the atomic weight and density of the
matrix
[AW_TiXAl,d_TiXAl] = AluminideCalc(X_Al,X_Ti);

% Calls CompositionCalc Function, which calculates the atomic percentages of the
matrix and reinforcement in the composite
[atper_TiXAl,atper_TiB2] =
CompositionCalc(AW_TiXAl,d_TiXAl,Vper_TiB2,X_Al,X_Ti);

% Calls abcdCalc Function, which calculates the a, b, c, and d multipliers for enthalpy
calculations
[a,b,c,d] = abcdCalc(X_Al,X_Ti,atper_TiXAl,atper_TiB2);

% Calls AluminideFrac Function, which calculates the fractions of each aluminide in the
matrix
[atper_Ti3Al,atper_TiAl,atper_Al3Ti] = AluminideFrac(X_Al,X_Ti);

% Physical Data

d_Al = 2.7;
M_Al = 26.98;

d_B = 2.34;
M_B = 10.811;
```

```
d_Ti = 4.50;
M_Ti = 47.9;

d_TiAl = 3.91;
M_TiAl = 75.2;

d_Ti3Al = 4.2;
M_Ti3Al = 170.68;

d_Al3Ti = 3.4;
M_Al3Ti = 128.84;

d_TiB2 = 4.50;
M_TiB2 = 69.522;

% Initialize vectors (speeds up iterative loops)

Hr_data = zeros(32021,1); % Enthalpy of Reactants
Hp_data = zeros(32021,1); % Enthalpy of Products
T_plot = zeros(32021,1); % Temperature

HAl = zeros(32021,1);
HTi = zeros(32021,1);

for j = 1:101

    Vper_TiAl = 100 - Vper_TiB2;

    T_ig = T_ig;

    Atper_TiB2 = atper_TiB2 * 100;
    Atper_TiAl = atper_TiAl * 100;
    Atper_Ti3Al = atper_Ti3Al * 100;
    Atper_Al3Ti = atper_Al3Ti * 100;

    moles_Al = b;
    moles_Ti = a + c;
    moles_B = d;
    moles_TiB2 = Atper_TiB2 / 100;
    moles_TiAl = Atper_TiAl * atper_TiXAl / 100;
    moles_Ti3Al = Atper_Ti3Al * atper_TiXAl / 100;
    moles_Al3Ti = Atper_Al3Ti * atper_TiXAl / 100;

    T1 = 298; % All temperatures in Kelvin
    Hp = 0;
    Hr = 0;
```

```
for i = 1:32021

    T = T1;
    % Aluminum Enthalpy Data
        if(T <= 933.44); % Solid Al
            H_Al = 7E-6*T.^2 + 0.0203*T - 6.6251;
        elseif(T <= 933.46); % Tm Al
            H_Al = 535.5*T - 499838.99;
        elseif(T <= 2790.8); % Liquid Al
            H_Al = 0.031707842*T - 0.738419701;
        elseif(T <= 2790.82) % Tvap Al
            H_Al = 14703.95*T - 41035696.14;
        else(T <= 3500); % Gas Al
            H_Al = 0.020828778 * T + 323.5161808;
        end

        % Titanium Enthalpy Data
        if (T <= 1165.99); % Alpha Ti
            H_Ti = 5E-06*T.^2 + 0.0223*T - 7.0815;
        elseif(T <= 1166.01); % Alpha - Beta Phase Change Ti
            H_Ti = 208.6 * T - 243199.732;
        elseif(T <= 1938.99); % Beta Ti
            H_Ti = 4E-06*T.^2 + 0.0197*T + 1.5395;
        elseif(T <= 1939.01) % Tm Ti
            H_Ti = 707.3 * T - 1371392.839;
        else(T <= 3500); % Liquid Ti
            H_Ti = 0.035563994 * T - 0.024608411;
        end

        % Amorphous Boron Enthalpy Data
        if (T <= 3500); % Amorphous B
            H_aB = -8E-10*T.^3 + 7E-06*T.^2 + 0.0125*T + 44.39;
        end

    % Crystalline Boron Enthalpy Data
        if (T <= 2349.99); % Beta B
            H_xB = 5E-06*T.^2 + 0.0223*T - 7.0815;
        elseif(T <= 1166.01); % Tm B
            H_xB = 2446.35 * T - 5748845.701;
        else(T <= 3500); % Liquid B
            H_xB = -8E-10*T.^3 + 7E-06*T.^2 + 0.0125*T + 44.39;
        end

    % TiAl Enthalpy Data
        if (T <= 1732.99); % Solid TiAl
```

```
            H_TiAl = 4E-06*T.^2 + 0.0518*T - 91.393;
        elseif(T <= 1733.01); % Tm TiAl
            H_TiAl = 3000*T - 5198958.48;
        else(T <= 3500); % Liquid TiAl
            H_TiAl = 0.066379929 * T - 43.5167915;
        end

    % Al3Ti Enthalpy Data
        if (T <= 1612.99); % Solid Al3Ti
            H_Al3Ti = 1E-05 * T.^2 + 0.0989 * T - 177.06;
        elseif(T <= 1613.01); % Tm Al3Ti
            H_Al3Ti = 4000 * T - 6451951.144;
        else(T <= 3500); % Liquid Al3Ti
            H_Al3Ti = 0.130180331*T - 121.1229617;
        end

    % Ti3Al Enthalpy Data (assumed to be the same at Al3Ti)
        if (T <= 1612.99); % Solid Ti3Al
            H_Ti3Al = 1E-05 * T.^2 + 0.0989 * T - 177.06;
        elseif(T <= 1613.01); % Tm Ti3Al
            H_Ti3Al = 4000 * T - 6451951.144;
        else(T <= 3500); % Liquid Ti3Al
            H_Ti3Al = 0.130180331*T - 121.1229617;
        end

    % TiB2 Enthalpy Data
        if (T <= 3192.99); % Solid TiB2
            H_TiB2 = 8E-06*T.^2 + 0.06*T - 344.58;
        elseif(T <= 3193.01); % Tm TiB2
            H_TiB2 = 5020.8 * T - 16031435.72;
        else(T <= 3500); % Liquid TiB2
            H_TiB2 = 0.108782674 * T - 318.4581817;
        end

    Hr = moles_Al * H_Al + moles_B * H_aB + moles_Ti * H_Ti;
    Hp = moles_TiB2 * H_TiB2 + moles_Al3Ti * H_Al3Ti + moles_TiAl * H_TiAl +
moles_Ti3Al * H_Ti3Al;

    HAl(i,1) = H_Al;
    HTi(i,1) = H_Ti;
    T_plot(i,1) = T;
    Hr_data(i,1) = Hr;
    Hp_data(i,1) = Hp;

    T1 = T1 + 0.1;
  end
```

```
end

X_Alp = 100* X_Al;
Vper_TiB2p = 100*Vper_TiB2;

wk1write('T_plot.csv',T_plot,1,0) % Writes the Temperature data to a CSV file
wk1write('Hr_data.csv',Hr_data,1,0) % Writes the Hr_data values to a CSV file
wk1write('Hp_data.csv',Hp_data,1,0) % Writes the Hp_data values to a CSV file

figure(1)
plot(T_plot, Hr_data)
hold on
plot(T_plot, Hp_data, 'g')
xlabel('Temperature, K')
ylabel('Enthalpy, kJ/mol')
title(['Ti-',int2str(X_Alp),'Al + ', int2str(Vper_TiB2p), 'V% TiB_{2}'])

% Calculate Adiabatic Temperature and DHrxn

index_T_ig_matrix = find(abs(T_plot-T_ig) < 1e-5);
TF = isempty(index_T_ig_matrix);
TF_1 = 0;
TF_2 = 0;
TF_3 = 0;
TF_4 = 0;
TF_5 = 0;

if(TF == 0)
   index_T_ig_matrix = index_T_ig_matrix;
end

if(TF == 1)
   index_T_ig_matrix = find(abs(Hp_data-Hr_T_ig) < .1);
   TF_1 = isempty(index_T_ig_matrix);
end

if(TF_1 == 1)
   index_T_ig_matrix = find(abs(Hp_data-Hr_T_ig) < 1);
   TF_2 = isempty(index_T_ig_matrix);
end

if(TF_2 == 1)
   index_T_ig_matrix = find(abs(Hp_data-Hr_T_ig) < 10);
   TF_3 = isempty(index_T_ig_matrix);
end
```

```
if(TF_3 == 1)
   index_T_ig_matrix = find(abs(Hp_data-Hr_T_ig) < 100);
   TF_4 = isempty(index_T_ig_matrix);
end

if(TF_4 == 1)
   index_T_ig_matrix = find(abs(Hp_data-Hr_T_ig) < 500);
   TF_5 = isempty(index_T_ig_matrix);
end

index_T_ig = max(index_T_ig_matrix);
Hr_T_ig = Hr_data(index_T_ig);

index_T_ad = find(abs(Hp_data-Hr_T_ig) < .01);

tf = isempty(index_T_ad);
tf_1 = 0;
tf_2 = 0;
tf_3 = 0;
tf_4 = 0;
tf_5 = 0;
tf_6 = 0;
tf_7 = 0;
dumb = 1;

if(tf == 0)
   index_T_ad = index_T_ad;
end

if(tf == 1)
   index_T_ad = find(abs(Hp_data-Hr_T_ig) < .1);
   tf_1 = isempty(index_T_ad);

      for kk = 1:500
         if(tf_1 == 1)
            index_T_ad = find(abs(Hp_data-Hr_T_ig) < dumb);
            tf_1 = isempty(index_T_ad);
            dumb = dumb + 1;
         end
      end

end

test = min(abs(Hp_data-Hr_T_ig));

min_index_T_ad = min(index_T_ad);
```

```
max_index_T_ad = max(index_T_ad);

test_min = abs(Hp_data(min_index_T_ad)-Hr_T_ig);
test_max = abs(Hp_data(max_index_T_ad)-Hr_T_ig);

if test == test_min
   index_T_ad = min_index_T_ad;
   T_Adiabatic_new = round(T_plot(index_T_ad));
   catcher = 1;
else
   index_T_ad = max_index_T_ad;
   T_Adiabatic_new = round(T_plot(index_T_ad));
   catcher = 2;
end

T_plot(min_index_T_ad);
T_plot(max_index_T_ad);

T_Adiabatic = round(T_plot(index_T_ad));

DHrxn = -(Hr_data(index_T_ig_matrix) - Hp_data(index_T_ig_matrix));
```

**AdiabaticCalc Subroutine**

```
function [Vper_TiB2_plot,T_ad_plot] = AdiabaticCalc(X_Al,T_ig)
%X_Al = .50;
%T_ig = 1000;
X_Ti = 1 - X_Al;

% Calls AluminideCalc Function, which calculates the atomic weight and density of the
matrix
[AW_TiXAl,d_TiXAl] = AluminideCalc(X_Al,X_Ti);

% Initialize vectors (speeds up iterative loops)

Hr_data = zeros(32021,1); % Enthalpy of Reactants
Hp_data = zeros(32021,1); % Enthalpy of Products
T_plot = zeros(32021,1); %

T_ad_plot = zeros(101,1);
Vper_TiB2_plot = zeros(101,1);
DHrxn_plot = zeros(101,1);

T_Adiabatic = 298;

Vper_TiB2 = 0;
```

```
%Hr_T_ig = 0;

for j = 1:101

    Vper_TiB2;

    % Physical Data

    d_Al = 2.7;
    M_Al = 26.98;

    d_B = 2.34;
    M_B = 10.811;

    d_Ti = 4.50;
    M_Ti = 47.9;

    d_TiAl = 3.91;
    M_TiAl = 75.2;

    d_Ti3Al = 4.2;
    M_Ti3Al = 170.68;

    d_Al3Ti = 3.4;
    M_Al3Ti = 128.84;

    d_TiB2 = 4.50;
    M_TiB2 = 69.522;

    T1 = 298; % All temperatures in Kelvin
    Hp = 0;
    Hr = 0;
    index_T_ad = 0;
    min_index_T_ad = 0;
    max_index_T_ad = 0;
    index_T_ig_matrix = 0;

    [atper_TiXAl,atper_TiB2] =
CompositionCalc(AW_TiXAl,d_TiXAl,Vper_TiB2,X_Al,X_Ti);
    [atper_Ti3Al,atper_TiAl,atper_Al3Ti] = AluminideFrac(X_Al,X_Ti);
    [a,b,c,d] = abcdCalc(X_Al,X_Ti,atper_TiXAl,atper_TiB2);

    Atper_TiB2 = atper_TiB2 * 100;
    Atper_TiAl = atper_TiAl * 100;
    Atper_Ti3Al = atper_Ti3Al * 100;
```

```
Atper_Al3Ti = atper_Al3Ti * 100;

moles_Al = b;
moles_Ti = a + c;
moles_B = d;
moles_TiB2 = atper_TiB2;
moles_TiAl = atper_TiAl * atper_TiXAl;
moles_Ti3Al = atper_Ti3Al * atper_TiXAl;
moles_Al3Ti = atper_Al3Ti * atper_TiXAl;

for i = 1:32021

   T = T1;
   % Aluminum Enthalpy Data
      if(T <= 933.44); % Solid Al
         H_Al = 7E-6*T.^2 + 0.0203*T - 6.6251;
      elseif(T <= 933.46); % Tm Al
         H_Al = 535.5*T - 499838.99;
      elseif(T <= 2790.8); % Liquid Al
         H_Al = 0.031707842*T - 0.738419701;
      elseif(T <= 2790.82) % Tvap Al
         H_Al = 14703.95*T - 41035696.14;
      else(T <= 3500); % Gas Al
         H_Al = 0.020828778 * T + 323.5161808;
      end

      % Titanium Enthalpy Data
      if (T <= 1165.99); % Alpha Ti
         H_Ti = 5E-06*T.^2 + 0.0223*T - 7.0815;
      elseif(T <= 1166.01); % Alpha - Beta Phase Change Ti
         H_Ti = 208.6 * T - 243199.732;
      elseif(T <= 1938.99); % Beta Ti
         H_Ti = 4E-06*T.^2 + 0.0197*T + 1.5395;
      elseif(T <= 1939.01) % Tm Ti
         H_Ti = 707.3 * T - 1371392.839;
      else(T <= 3500); % Liquid Ti
         H_Ti = 0.035563994 * T - 0.024608411;
      end

      % Amorphous Boron Enthalpy Data
      if (T <= 3500); % Amorphous B
         H_aB = -8E-10*T.^3 + 7E-06*T.^2 + 0.0125*T + 44.39;
      end

   % Crystalline Boron Enthalpy Data
      if (T <= 2349.99); % Beta B
```

```
        H_xB = 5E-06*T.^2 + 0.0223*T - 7.0815;
    elseif(T <= 1166.01); % Tm B
        H_xB = 2446.35 * T - 5748845.701;
    else(T <= 3500); % Liquid B
        H_xB = -8E-10*T.^3 + 7E-06*T.^2 + 0.0125*T + 44.39;
    end

% TiAl Enthalpy Data
    if (T <= 1732.99); % Solid TiAl
        H_TiAl = 4E-06*T.^2 + 0.0518*T - 91.393;
    elseif(T <= 1733.01); % Tm TiAl
        H_TiAl = 3000*T - 5198958.48;
    else(T <= 3500); % Liquid TiAl
        H_TiAl = 0.066379929 * T - 43.5167915;
    end

% Al3Ti Enthalpy Data
    if (T <= 1612.99); % Solid Al3Ti
        H_Al3Ti = 1E-05 * T.^2 + 0.0989 * T - 177.06;
    elseif(T <= 1613.01); % Tm Al3Ti
        H_Al3Ti = 4000 * T - 6451951.144;
    else(T <= 3500); % Liquid Al3Ti
        H_Al3Ti = 0.130180331*T - 121.1229617;
    end

% Ti3Al Enthalpy Data (assumed to be the same at Al3Ti)
    if (T <= 1612.99); % Solid Ti3Al
        H_Ti3Al = 1E-05 * T.^2 + 0.0989 * T - 177.06;
    elseif(T <= 1613.01); % Tm Ti3Al
        H_Ti3Al = 4000 * T - 6451951.144;
    else(T <= 3500); % Liquid Ti3Al
        H_Ti3Al = 0.130180331*T - 121.1229617;
    end

% TiB2 Enthalpy Data
    if (T <= 3192.99); % Solid TiB2
        H_TiB2 = 8E-06*T.^2 + 0.06*T - 344.58;
    elseif(T <= 3193.01); % Tm TiB2
        H_TiB2 = 5020.8 * T - 16031435.72;
    else(T <= 3500); % Liquid TiB2
        H_TiB2 = 0.108782674 * T - 318.4581817;
    end

Hr = moles_Al * H_Al + moles_B * H_aB + moles_Ti * H_Ti;
Hp = moles_TiB2 * H_TiB2 + moles_Al3Ti * H_Al3Ti + moles_TiAl * H_TiAl +
moles_Ti3Al * H_Ti3Al;
```

```
    T_plot(i,1) = T;
    Hr_data(i,1) = Hr;
    Hp_data(i,1) = Hp;

    T1 = T1 + 0.1;
end

%Hr_T_ig =

index_T_ig_matrix = find(abs(T_plot-T_ig) < 1e-5);
TF = isempty(index_T_ig_matrix);
TF_1 = 0;
TF_2 = 0;
TF_3 = 0;
TF_4 = 0;
TF_5 = 0;

if(TF == 0)
    index_T_ig_matrix = index_T_ig_matrix;
end

if(TF == 1)
    index_T_ig_matrix = find(abs(Hp_data-Hr_T_ig) < .1);
    TF_1 = isempty(index_T_ig_matrix);
end

if(TF_1 == 1)
    index_T_ig_matrix = find(abs(Hp_data-Hr_T_ig) < 1);
    TF_2 = isempty(index_T_ig_matrix);
end

if(TF_2 == 1)
    index_T_ig_matrix = find(abs(Hp_data-Hr_T_ig) < 10);
    TF_3 = isempty(index_T_ig_matrix);
end

if(TF_3 == 1)
    index_T_ig_matrix = find(abs(Hp_data-Hr_T_ig) < 100);
    TF_4 = isempty(index_T_ig_matrix);
end

if(TF_4 == 1)
    index_T_ig_matrix = find(abs(Hp_data-Hr_T_ig) < 500);
    TF_5 = isempty(index_T_ig_matrix);
end
```

```
index_T_ig = max(index_T_ig_matrix);
Hr_T_ig = Hr_data(index_T_ig);

index_T_ad = find(abs(Hp_data-Hr_T_ig) < .01);

tf = isempty(index_T_ad);
tf_1 = 0;
tf_2 = 0;
tf_3 = 0;
tf_4 = 0;
tf_5 = 0;
tf_6 = 0;
tf_7 = 0;
dumb = 1;

if(tf == 0)
   index_T_ad = index_T_ad;
end

if(tf == 1)
   index_T_ad = find(abs(Hp_data-Hr_T_ig) < .1);
   tf_1 = isempty(index_T_ad);

      for kk = 1:500
         if(tf_1 == 1)
            index_T_ad = find(abs(Hp_data-Hr_T_ig) < dumb);
            tf_1 = isempty(index_T_ad);
            dumb = dumb + 1;
         end
      end
end

test = min(abs(Hp_data-Hr_T_ig));

min_index_T_ad = min(index_T_ad);
max_index_T_ad = max(index_T_ad);

test_min = abs(Hp_data(min_index_T_ad)-Hr_T_ig);
test_max = abs(Hp_data(max_index_T_ad)-Hr_T_ig);

if test == test_min
   index_T_ad = min_index_T_ad;
   T_Adiabatic_new = round(T_plot(index_T_ad));
   catcher = 1;
else
```

```
        index_T_ad = max_index_T_ad;
        T_Adiabatic_new = round(T_plot(index_T_ad));
        catcher = 2;
    end

    T_plot(min_index_T_ad);
    T_plot(max_index_T_ad);

    T_Adiabatic = round(T_plot(index_T_ad));

    T_ad_plot(j,1) = T_Adiabatic;

    Vper_TiB2_plot(j,1) = Vper_TiB2;

    DHrxn = -(Hr_data(index_T_ig_matrix) - Hp_data(index_T_ig_matrix));

    DHrxn_plot(j,1) = DHrxn;

    Vper_TiB2 = Vper_TiB2 + 0.01;
end

Vper_TiB2_plot = 100 * Vper_TiB2_plot;
X_Alp = 100* X_Al;

figure(1)
plot(Vper_TiB2_plot,T_ad_plot)
xlabel('Volume Percent of TiB_{2} in Product')
ylabel('Calculated Adiabatic Temperature, K')
title(['Ti-',int2str(X_Alp),'Al + V% TiB_{2}'])
axis([0 1 1600 3600])

hold on
figure(2)
plot(Vper_TiB2_plot,DHrxn_plot)
xlabel('Volume Percent of TiB_{2} in Product')
ylabel('\DeltaH_{rxn}, J/mole')
title(['Ti-',int2str(X_Alp),'Al + V% TiB_{2}'])
axis([0 1 -450 0])

output = [Vper_TiB2_plot T_ad_plot DHrxn_plot];

wk1write('AdiabaticTempPlot.csv',output,1,1) % Writes the Adiabatic Temperature data
to a CSV file
```

**TadHrxnAllXs Subroutine**

```
function [X_Al_plot,T_Ad_output,DHrxn_output] = TadHrxnAllXs(Vper_TiB2,T_ig)

X_Al_plot = zeros(51,1);
T_Ad_output = zeros(51,1);
DHrxn_output = zeros(51,1);

X_Al = 0.25;

for ii = 1:52

if ii < 52
X_Al
X_Ti = 1 - X_Al;

% Calls AluminideCalc Function, which calculates the atomic weight and density of the
matrix
[AW_TiXAl,d_TiXAl] = AluminideCalc(X_Al,X_Ti);

% Calls CompositionCalc Function, which calculates the atomic percentages of the
matrix and reinforcement in the composite
[atper_TiXAl,atper_TiB2] =
CompositionCalc(AW_TiXAl,d_TiXAl,Vper_TiB2,X_Al,X_Ti);

% Calls abcdCalc Function, which calculates the a, b, c, and d multipliers for enthalpy
calculations
[a,b,c,d] = abcdCalc(X_Al,X_Ti,atper_TiXAl,atper_TiB2);

% Calls AluminideFrac Function, which calculates the fractions of each aluminide in the
matrix
[atper_Ti3Al,atper_TiAl,atper_Al3Ti] = AluminideFrac(X_Al,X_Ti);

% Physical Data

d_Al = 2.7;
M_Al = 26.98;

d_B = 2.34;
M_B = 10.811;

d_Ti = 4.50;
M_Ti = 47.9;

d_TiAl = 3.91;
M_TiAl = 75.2;
```

```
d_Ti3Al = 4.2;
M_Ti3Al = 170.68;

d_Al3Ti = 3.4;
M_Al3Ti = 128.84;

d_TiB2 = 4.50;
M_TiB2 = 69.522;

% Initialize vectors (speeds up iterative loops)

Hr_data = zeros(32021,1); % Enthalpy of Reactants
Hp_data = zeros(32021,1); % Enthalpy of Products
T_plot = zeros(32021,1); % Temperature

HAl = zeros(32021,1);
HTi = zeros(32021,1);

for j = 1:101

    Vper_TiAl = 100 - Vper_TiB2;

    T_ig = T_ig;

    Atper_TiB2 = atper_TiB2 * 100;
    Atper_TiAl = atper_TiAl * 100;
    Atper_Ti3Al = atper_Ti3Al * 100;
    Atper_Al3Ti = atper_Al3Ti * 100;

    moles_Al = b;
    moles_Ti = a + c;
    moles_B = d;
    moles_TiB2 = Atper_TiB2 / 100;
    moles_TiAl = Atper_TiAl * atper_TiXAl / 100;
    moles_Ti3Al = Atper_Ti3Al * atper_TiXAl / 100;
    moles_Al3Ti = Atper_Al3Ti * atper_TiXAl / 100;

    T1 = 298; % All temperatures in Kelvin
    Hp = 0;
    Hr = 0;

    for i = 1:32021

        T = T1;
        % Aluminum Enthalpy Data
```

```
    if(T <= 933.44); % Solid Al
       H_Al = 7E-6*T.^2 + 0.0203*T - 6.6251;
    elseif(T <= 933.46); % Tm Al
       H_Al = 535.5*T - 499838.99;
    elseif(T <= 2790.8); % Liquid Al
       H_Al = 0.031707842*T - 0.738419701;
    elseif(T <= 2790.82) % Tvap Al
       H_Al = 14703.95*T - 41035696.14;
    else(T <= 3500); % Gas Al
       H_Al = 0.020828778 * T + 323.5161808;
    end

    % Titanium Enthalpy Data
    if (T <= 1165.99); % Alpha Ti
       H_Ti = 5E-06*T.^2 + 0.0223*T - 7.0815;
    elseif(T <= 1166.01); % Alpha - Beta Phase Change Ti
       H_Ti = 208.6 * T - 243199.732;
    elseif(T <= 1938.99); % Beta Ti
       H_Ti = 4E-06*T.^2 + 0.0197*T + 1.5395;
    elseif(T <= 1939.01) % Tm Ti
       H_Ti = 707.3 * T - 1371392.839;
    else(T <= 3500); % Liquid Ti
       H_Ti = 0.035563994 * T - 0.024608411;
    end

    % Amorphous Boron Enthalpy Data
    if (T <= 3500); % Amorphous B
       H_aB = -8E-10*T.^3 + 7E-06*T.^2 + 0.0125*T + 44.39;
    end

% Crystalline Boron Enthalpy Data
    if (T <= 2349.99); % Beta B
       H_xB = 5E-06*T.^2 + 0.0223*T - 7.0815;
    elseif(T <= 1166.01); % Tm B
       H_xB = 2446.35 * T - 5748845.701;
    else(T <= 3500); % Liquid B
       H_xB = -8E-10*T.^3 + 7E-06*T.^2 + 0.0125*T + 44.39;
    end

% TiAl Enthalpy Data
    if (T <= 1732.99); % Solid TiAl
       H_TiAl = 4E-06*T.^2 + 0.0518*T - 91.393;
    elseif(T <= 1733.01); % Tm TiAl
       H_TiAl = 3000*T - 5198958.48;
    else(T <= 3500); % Liquid TiAl
       H_TiAl = 0.066379929 * T - 43.5167915;
```

```
        end

    % Al3Ti Enthalpy Data
        if (T <= 1612.99); % Solid Al3Ti
            H_Al3Ti = 1E-05 * T.^2 + 0.0989 * T - 177.06;
        elseif(T <= 1613.01); % Tm Al3Ti
            H_Al3Ti = 4000 * T - 6451951.144;
        else(T <= 3500); % Liquid Al3Ti
            H_Al3Ti = 0.130180331*T - 121.1229617;
        end

    % Ti3Al Enthalpy Data (assumed to be the same at Al3Ti)
        if (T <= 1612.99); % Solid Ti3Al
            H_Ti3Al = 1E-05 * T.^2 + 0.0989 * T - 177.06;
        elseif(T <= 1613.01); % Tm Ti3Al
            H_Ti3Al = 4000 * T - 6451951.144;
        else(T <= 3500); % Liquid Ti3Al
            H_Ti3Al = 0.130180331*T - 121.1229617;
        end

    % TiB2 Enthalpy Data
        if (T <= 3192.99); % Solid TiB2
            H_TiB2 = 8E-06*T.^2 + 0.06*T - 344.58;
        elseif(T <= 3193.01); % Tm TiB2
            H_TiB2 = 5020.8 * T - 16031435.72;
        else(T <= 3500); % Liquid TiB2
            H_TiB2 = 0.108782674 * T - 318.4581817;
        end

    Hr = moles_Al * H_Al + moles_B * H_aB + moles_Ti * H_Ti;
    Hp = moles_TiB2 * H_TiB2 + moles_Al3Ti * H_Al3Ti + moles_TiAl * H_TiAl +
moles_Ti3Al * H_Ti3Al;

    HAl(i,1) = H_Al;
    HTi(i,1) = H_Ti;
    T_plot(i,1) = T;
    Hr_data(i,1) = Hr;
    Hp_data(i,1) = Hp;

    T1 = T1 + 0.1;
  end
end

% Calculate Adiabatic Temperature and DHrxn

index_T_ig_matrix = find(abs(T_plot-T_ig) < 1e-5);
```

```
TF = isempty(index_T_ig_matrix);
TF_1 = 0;
TF_2 = 0;
TF_3 = 0;
TF_4 = 0;
TF_5 = 0;

if(TF == 0)
   index_T_ig_matrix = index_T_ig_matrix;
end

if(TF == 1)
   index_T_ig_matrix = find(abs(Hp_data-Hr_T_ig) < .1);
   TF_1 = isempty(index_T_ig_matrix);
end

if(TF_1 == 1)
   index_T_ig_matrix = find(abs(Hp_data-Hr_T_ig) < 1);
   TF_2 = isempty(index_T_ig_matrix);
end

if(TF_2 == 1)
   index_T_ig_matrix = find(abs(Hp_data-Hr_T_ig) < 10);
   TF_3 = isempty(index_T_ig_matrix);
end

if(TF_3 == 1)
   index_T_ig_matrix = find(abs(Hp_data-Hr_T_ig) < 100);
   TF_4 = isempty(index_T_ig_matrix);
end

if(TF_4 == 1)
   index_T_ig_matrix = find(abs(Hp_data-Hr_T_ig) < 500);
   TF_5 = isempty(index_T_ig_matrix);
end

index_T_ig = max(index_T_ig_matrix);
Hr_T_ig = Hr_data(index_T_ig);

index_T_ad = find(abs(Hp_data-Hr_T_ig) < .01);

tf = isempty(index_T_ad);
tf_1 = 0;
tf_2 = 0;
tf_3 = 0;
tf_4 = 0;
```

```
tf_5 = 0;
tf_6 = 0;
tf_7 = 0;
dumb = 1;

if(tf == 0)
   index_T_ad = index_T_ad;
end

if(tf == 1)
   index_T_ad = find(abs(Hp_data-Hr_T_ig) < .1);
   tf_1 = isempty(index_T_ad);

      for kk = 1:500
         if(tf_1 == 1)
            index_T_ad = find(abs(Hp_data-Hr_T_ig) < dumb);
            tf_1 = isempty(index_T_ad);
            dumb = dumb + 1;
         end
      end

end

test = min(abs(Hp_data-Hr_T_ig));

min_index_T_ad = min(index_T_ad);
max_index_T_ad = max(index_T_ad);

test_min = abs(Hp_data(min_index_T_ad)-Hr_T_ig);
test_max = abs(Hp_data(max_index_T_ad)-Hr_T_ig);

if test == test_min
   index_T_ad = min_index_T_ad;
   T_Adiabatic_new = round(T_plot(index_T_ad));
   catcher = 1;
else
   index_T_ad = max_index_T_ad;
   T_Adiabatic_new = round(T_plot(index_T_ad));
   catcher = 2;
end

T_plot(min_index_T_ad);
T_plot(max_index_T_ad);

T_Adiabatic = round(T_plot(index_T_ad));
```

```
DHrxn = -(Hr_data(index_T_ig_matrix) - Hp_data(index_T_ig_matrix));

T_Ad_output(ii,1) = T_Adiabatic;
DHrxn_output(ii,1) = DHrxn;

X_Al_plot(ii,1) = 100 * X_Al;

X_Al = X_Al + 0.01;

if ii == 50
   output = [X_Al_plot T_Ad_output DHrxn_output];
   wk1write('T_Ad_H_f_xs50.csv',output,1,1) % Writes the Adiabatic Temperature and
Heat of Formation data to a CSV file
end

else
   X_Al;
end
end

output = [X_Al_plot T_Ad_output DHrxn_output];
wk1write('T_Ad_H_f_xs51.csv',output,1,1) % Writes the Adiabatic Temperature and
Heat of Formation data to a CSV file

V_per_TiB2 = 100 * Vper_TiB2;

figure(1)
plot(X_Al_plot,T_Ad_output)
xlabel('x in Ti-xAl, at% Al')
ylabel('T_[13], K')
title(['Ti-xAl + ',int2str(V_per_TiB2),'V% TiB_{2}'])

hold on

figure(2)
plot(X_Al_plot,DHrxn_output)
xlabel('x in Ti-xAl, at% Al')
ylabel('\DeltaH_{rxn}, J/mole')
title(['Ti-xAl + ',int2str(V_per_TiB2),'V% TiB_{2}'])
```

# 8 References


1. Franklin, J., *In-Situ Synthesis of Piezoelectric-Reinforced Metal Matrix Composites*, in *Materials Science and Engineering*. 2003, Virginia Polytechnic Institute and State University: Blacksburg, VA. p. 110.
2. Martin, R., et al., *Microstructure/processing relationships in reaction-synthesized titanium aluminide intermetallic matrix composites.* Metallurgical & Materials Transactions A-Physical Metallurgy & Materials Science, 2002. **33**(8): p. 2747-2753.
3. Dong, S., et al., *Synthesis of intermetallic NiAl by SHS reaction using coarse-grained nickel and ultrafine-grained aluminum produced by wire electrical explosion.* Intermetallics, 2002. **10**(3): p. 217-223.
4. Moore, J.J. and H.J. Feng, *Combustion synthesis of advanced materials: Part I. Reaction parameters.* Progress in Materials Science, 1995. **39**(4-5): p. 243-273.
5. Yeh, C.L. and S.H. Su, *In situ formation of TiAl-TiB2 composite by SHS.* Journal of Alloys and Compounds, 2006. **407**(1-2): p. 150-156.
6. Mossino, P., *Some aspects in self-propagating high-temperature synthesis.* Ceramics International, 2004. **30**(3): p. 311-332.
7. Munir, Z.A. and U. Anselmi-Tamburini, *Self-propagating exothermic reactions: The synthesis of high-temperature materials by combustion.* Materials Science Reports, 1989. **3**(7-8): p. 277-365.
8. Murray, J.L., *Aluminum-Titanium Phase Diagram*, in *Metals Handbook Desk Edition [ASM Handbooks Online]*. 1987.
9. Muffo, P., *percent.m*. 2003, Unpublished.
10. Kampe, S.L., *Personal Communication*, E. Jeffers, Editor. 2006.
11. Chiu, L.H., D.C. Nagle, and L.A. Bonney, *Thermal Analysis of Self-Propagating High-Temperature Reactions in Titanium, Boron, and Aluminum Powder Compacts.* Metallurgical & Materials Transactions A-Physical Metallurgy & Materials Science, 1999. **30A**(3): p. 781-788.
12. Barin, I., *Thermomechanical Data of Pure Substances*. 2nd ed. 1993, Weinheim: VCH.
13. Jokisaari, J.R., S. Bhaduri, and S.B. Bhaduri, *Microwave activated combustion synthesis of titanium aluminides.* Materials Science and Engineering A, 2005. **394**(1-2): p. 385-392.

# 9 VITA

Elizabeth Jeffers was born and raised in Gaithersburg, Maryland. She began playing volleyball at a young age, and after graduating from Gaithersburg High School in 2000 she had the opportunity to walk-on to the Virginia Tech Varsity Volleyball team. After a year and a half of playing a varsity sport and being an engineering student, Elizabeth decided to focus on her studies in Materials Science and Engineering and left the volleyball team. She has had the opportunity to work at INTERMET – Radford Foundry as a Quality Associate and at the Naval Surface Warfare Center – Carderock Division in the Fatigue and Fracture Branch during her time as an undergraduate. After graduating from the MSE Department in December 2004, Elizabeth decided to stay on for her master's degree. Elizabeth was a recipient of the Aerojet Propulsion Fellowship for the 2005-2006 academic year and had the opportunity to work at Aerojet in the structures group. Elizabeth has accepted a job offer with Precision Castparts Corporation and will begin at their Special Metals facility in New Hartford, NY in late October.

September 2006